agso RESEARCH NEWSLETTER

'Geoscience for Australia's Future'

Number 24 May 1996

Gold targets in the northeast Duketon 1:250 000 Sheet area, Eastern Goldfields, Western Australia

Alastair J. Stewart[1]

The northeast Duketon 1:250000 Sheet area (Fig. 1) lies in the north of the Eastern Goldfields of Western Australia. It adjoins several areas which are currently the focus of some of the most active gold exploration in the Goldfields. These areas include the Dingo Range and Yandal greenstone belts to the west, and the Duketon greenstone belt to the south. Recently opened major mines at Bronzewing, Jundee, and Mount McClure in the Yandal belt show that gold is not restricted to the large greenstone areas of the Kalgoorlie–Leonora region. The integration of high-quality aeromagnetic data, acquired in 1993, with data derived from geological

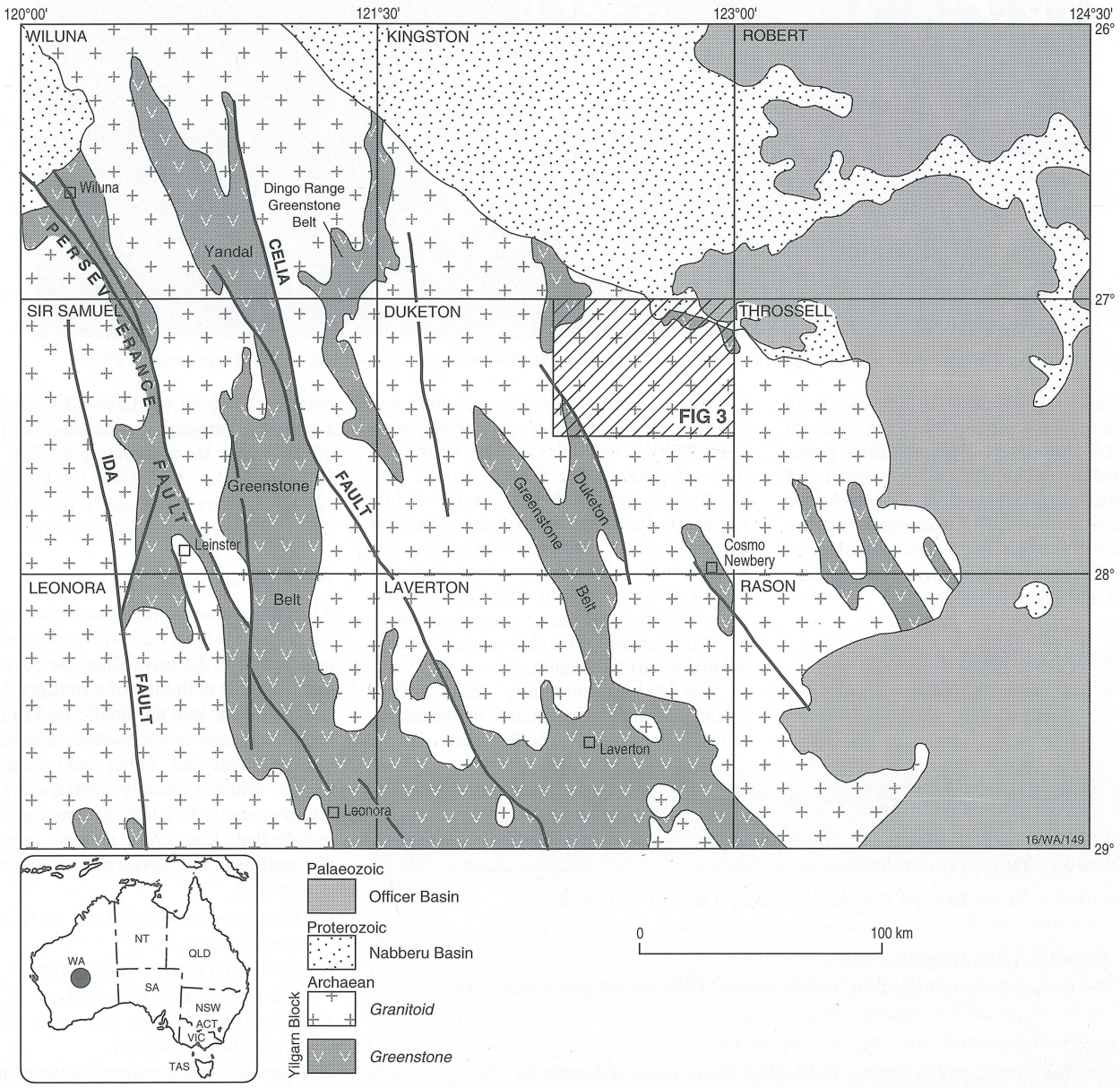

Fig. 1. Regional geology of the northern part of the Eastern Goldfields Province, Western Australia (after Myers & Hocking, compilers, 1988: Geological map of Western Australia, 1:2 500 000; Geological Survey of Western Australia). The northeast Duketon 1:250 000 Sheet area is hachured.

Table of contents on page 2

AGSO

Australian Geological Survey Organisation

a research organisation of the Department of Primary Industries & Energy

AGSO JUBILEE 1946-96

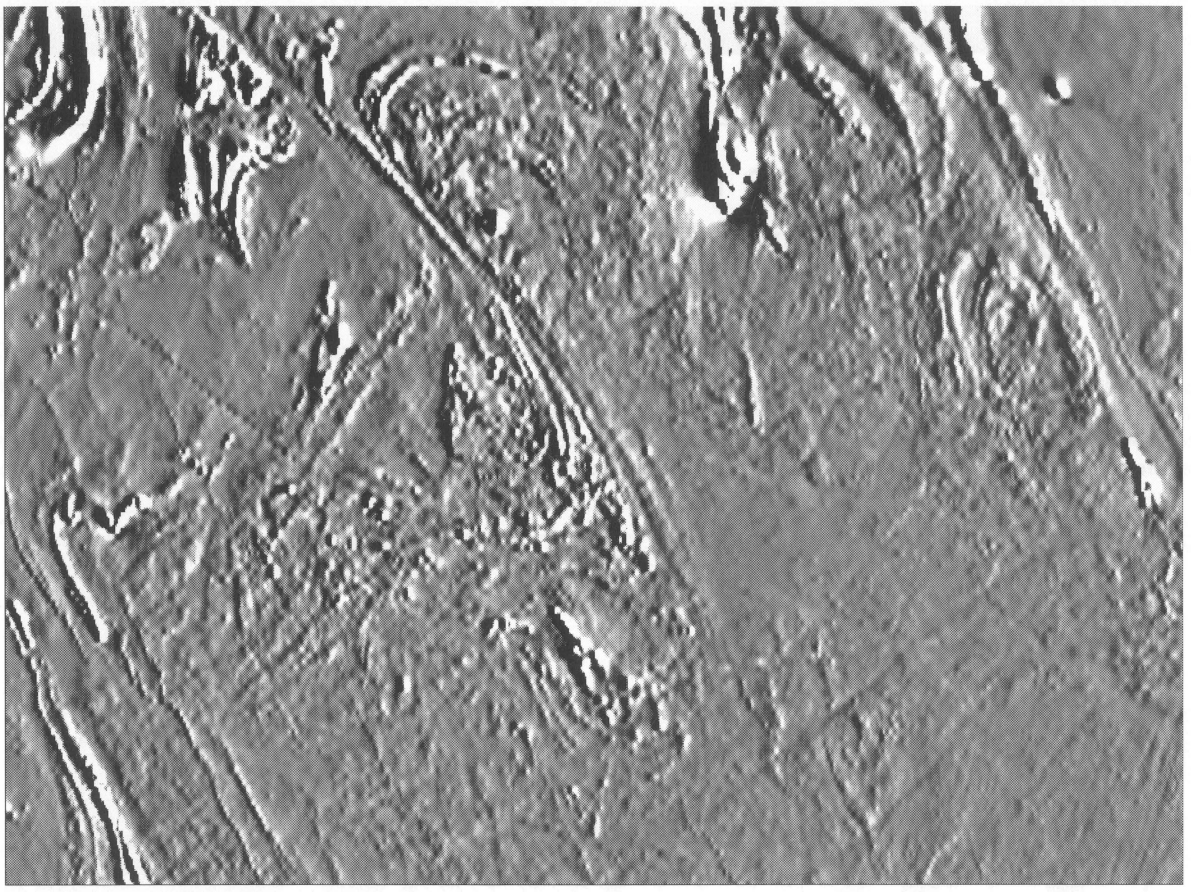

Fig. 2. Total magnetic intensity image of the northeast Duketon 1:250 000 Sheet area (400-m line spacing; same area as Fig. 3).

mapping and sampling in 1994 — both National Geoscience Mapping Accord (NGMA) initiatives — has identified possible gold targets in a largely concealed and previously unrecognised greenstone belt in northeast Duketon. The area concerned has produced no base or precious metals, and has hitherto been regarded as composed almost entirely of granitoid.

Regional setting

Most of the northeast Duketon 1:250 000 Sheet area lies within the Archaean Yilgarn Craton. Sedimentary rocks occupy the northeast corner (part of the Palaeoproterozoic Nabberu Basin), and crop out as widely scattered Permian outliers (vestiges of the Officer Basin). The Yilgarn rocks are greenstone, granitoid, and gneiss of late Archaean age. The greenstones comprise mafic volcanics, shale, and banded iron formation, with minor mafic intrusions in the southwest and ultramafic schist in the northwest. Granitoid and lesser amounts of previously unrecognised banded gneiss make up the major part of the area.

The Palaeoproterozoic rocks reflect siliciclastic shelf sedimentation on the margin of the Yilgarn Craton. The Permian rocks are bouldery siltstone and feldspathic sandstone assigned to the glacigene Paterson Formation of the Officer Basin (Bunting & Chin 1979: Duketon, W.A. — 1:250000 Geological Series Explanatory Notes, SG51/14, Geological Survey of Western Australia, Perth).

Archaean geology

Although Archaean rocks underlie about 85 per cent of the area, their widely separated exposures and an extensive Cainozoic cover have precluded the definition of a stratigraphic sequence. Mafic and ultramafic rocks include metamorphosed basalt, gabbro, dolerite, and talc–carbonate rock. Other rocks are quartz–biotite schist (possibly metadacite), and quartz–muscovite schist. Sedimentary rocks include shale, slate, chert, quartzite, cross-bedded sandstone, and banded iron formation. The presence of:

- blue–green amphibole in mafic metaigneous rocks,
- biotite and muscovite in schist,
- talc in ultramafic rock, and
- interstitial chlorite and white mica in plagioclase in dolerite

indicates low-grade metamorphism (middle greenschist to transitional greenschist–amphibolite facies).

Almost all granitoid exposures are heavily weathered monzogranite. Xenoliths and rafts of banded gneiss in granitoid form a discontinuous north–south belt extending for some 30 km in the west of the area.

In this issue:

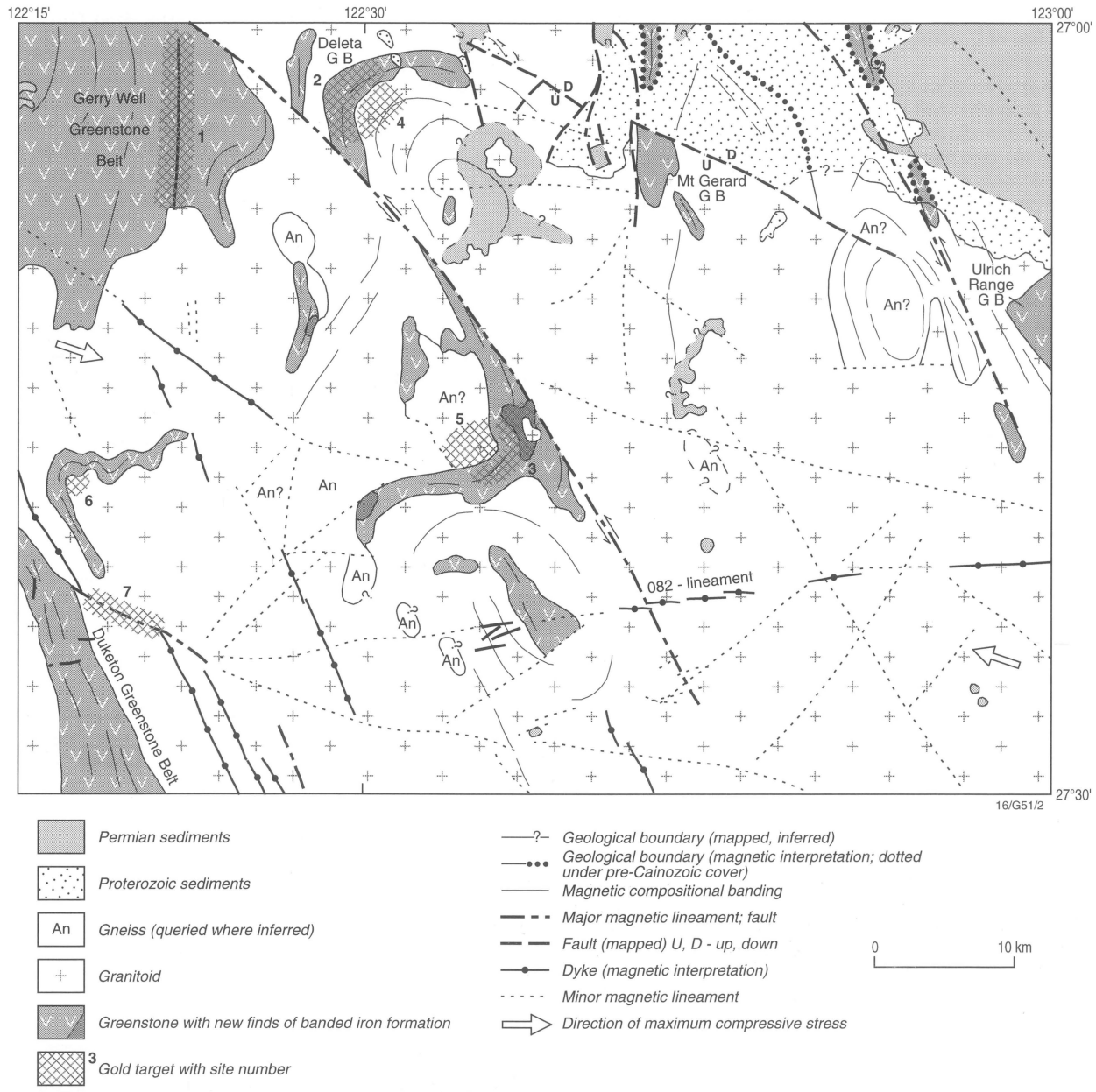

Fig. 3. Solid geology map of the northeast Duketon 1:250 000 Sheet area compiled from geological mapping by the author and from interpretation of aeromagnetic data by A.J. Whitaker and P. Lyons (both of AGSO) and the author.

Structure

Imagery derived from aeromagnetic data (Fig. 2) indicates the presence of several masses of compositionally banded, strongly magnetic rock in areas almost entirely concealed by Cainozoic cover. Three such masses coincide with basalt and newly recognised outcrops of banded iron formation; the other concealed masses are hence interpreted as greenstone also.

Two major lineaments strike northwest across the area (Fig. 3). The western lineament cuts one of the previously unknown greenstone belts* into two parts laterally offset by 15–30 km; bending and drag indicate that it is a major sinistral shear zone. Sinistral offset along the eastern lineament appears to be about 15 km, if the two small, strongly magnetic bodies located either side of the eastern lineament — respectively 8 km north-northwest and 5 km southwest of the Ulrich Range greenstone belt — were once one body.

Minor lineaments cut the granitoid and greenstone outcrops, and are probably major fractures, with or without dyke fillings. They tend to have a more latitudinal strike than the major northwest-striking shear zones. Portions of one lineament striking 082° in the southeast are pulled apart and apparently rotated clockwise, suggesting that they represent tension gashes formed during dextral shear.

The major and minor lineaments are interpreted to be of different ages, but older than Palaeoproterozoic. The northwest-striking shear zones are older, as movement along the one that segments the Deleta greenstone belt had ceased before the 082° lineament formed. The roughly latitudinal fractures may have formed during waning of the tectonism that produced the northwest shear zones, the same stress-field creating both sets of dislocations. If so, the sinistral slip along the northwest shear zone through the Deleta greenstone belt, and the dextral slip along the 082° lineament in the southeast, indicate that the maximum compressive stress in northeast Duketon was oriented west-northwest during the latest Archaean.

Possible gold targets

The discovery of banded iron formation and basalt exposures in northeast Duketon in 1994, and the subsurface extent of these rocks indicated by the 400-m-spaced aeromagnetic data acquired in 1993, suggest there is significant potential for gold deposits in the area. The greenstones were metamorphosed under conditions ranging from middle greenschist facies up to the greenschist–amphibolite transition, so they could be expected to carry breccia-, vein-array-, and shear-zone-hosted epigenetic gold lodes (Groves et al. 1995: *In*:

Coward, M.P. & Ries, A.C. (editors), Geological Society of London, Special Publication 95, 155–172).

Breccia-type lodes are a possibility in the Gerry Well greenstone belt in the northwest, where chlorite in mafic rocks could indicate a very low-grade metamorphic environment suitable for deposits of the Wiluna and Mount Pleasant types. No faults where breccias could be sought have been recognised in this poorly exposed belt, but a major magnetic lineament strikes north through it, and a minor magnetic lineament strikes northwest through the southern part of it. The lineaments are probably faults, and warrant investigation for breccias (site 1, Fig. 3).

Shear-zone deposits in stockworks or parallel sets of quartz veins accompanied by alteration zones are possible in competent rocks in the area. Sinusoidal bending of the two parts of the Deleta greenstone belt demonstrates the effect of considerable deformation along the shear zone separating them. Folding of moderately competent rock types such as dolerite and banded iron formation during the shearing could have favoured the emplacement of quartz-vein stockworks (sites 2 and 3, Fig. 3) as found at Mount Charlotte, Lancefield, Victory Defiance, Sons of Gwalia, Hill 50, and Mount Morgan.

Sites of low mean stress favouring fluid flow and hence gold deposition can be predicted near the margins of rigid rock bodies subjected to the far-field west-northwest-oriented compressive stress inferred in this area (Ridley 1993: Ore Geology Reviews, 8, 23-37; Groves et al. 1995: op. cit.). Possible sites in northeast Duketon are:

- the granitoid juxtaposed against the concave regions of the Deleta greenstone belt (both parts; sites 4 and 5, Fig. 3) and the unnamed greenstone belt (site 6) in the west; the greenstone belts are folded, and the more rigid granitoid in the hinge regions might have deflected the stress field and produced regions of heterogeneous stress and low mean stress, as at Granny Smith; and
- the north-northwesterly striking dyke-filled fracture in the southwest (site 7) that appears to be sinistrally offset by several kilometres along a minor lineament; the dilational jog so formed could have dilated during later movement along the minor lineament, and focused ore-fluid flow, as at the Wiluna and Mount Pleasant deposits.

Relevant maps and data

New 1:100 000-scale geological maps (Tate, Urarey, and De La Poer) of the northern half of the Duketon 1:250 000 Sheet area are available from AGSO in digital form and as coloured on-demand paper prints, together with an accompanying report (see announcement in AUS.GEO News 32, for February 1996, p. 6). Geophysical data for the Duketon Sheet area have been previously released.+

[1] AGSO Division of Regional Geology & Minerals, GPO Box 378, Canberra, ACT 2601; tel. +61 6 249 9666, fax +61 6 249 9983.

* Here named the Deleta greenstone belt after Deleta homestead, which is located at the margin of the northern portion of the belt.

+ Total magnetic intensity (TMI) contours and profiles, total-count contours, and flight lines; magnetic and gamma-ray spectrometric digital data (point-located and gridded); and pixel-image maps (TMI in colour and grey-scale), all at 1:250 000 (see AUS.GEO News 23, for August 1994, p. 10, and 25, for December 1994, p. 6). Digital-elevation-model (DEM) data (point-located and gridded) and contours were released in February 1996 (see AUS.GEO News 32, for February 1996, p. 10). The Duketon Sheet area also forms part of gradient enhanced colour and grey-scale 1:1 000 000 pixel-image TMI maps reduced to the pole for the northern Eastern Goldfields (see AUS.GEO News 30, for October 1995, p.14).

How ancient is the Bungle Bungle Range of the East Kimberley, Western Australia?

David H. Blake[1]

The Bungle Bungle Range rises up to 640 m above sea level and 380 m above a surrounding sand plain to form the spectacular scenic attraction of Purnululu National Park. An illustrated information booklet on this park ('Bungle Bungle Range', by Hoatson et al.) is currently being prepared by AGSO in collaboration with the Geological Survey of Western Australia (GSWA) and the Department of Conservation & Land Management of Western Australia.

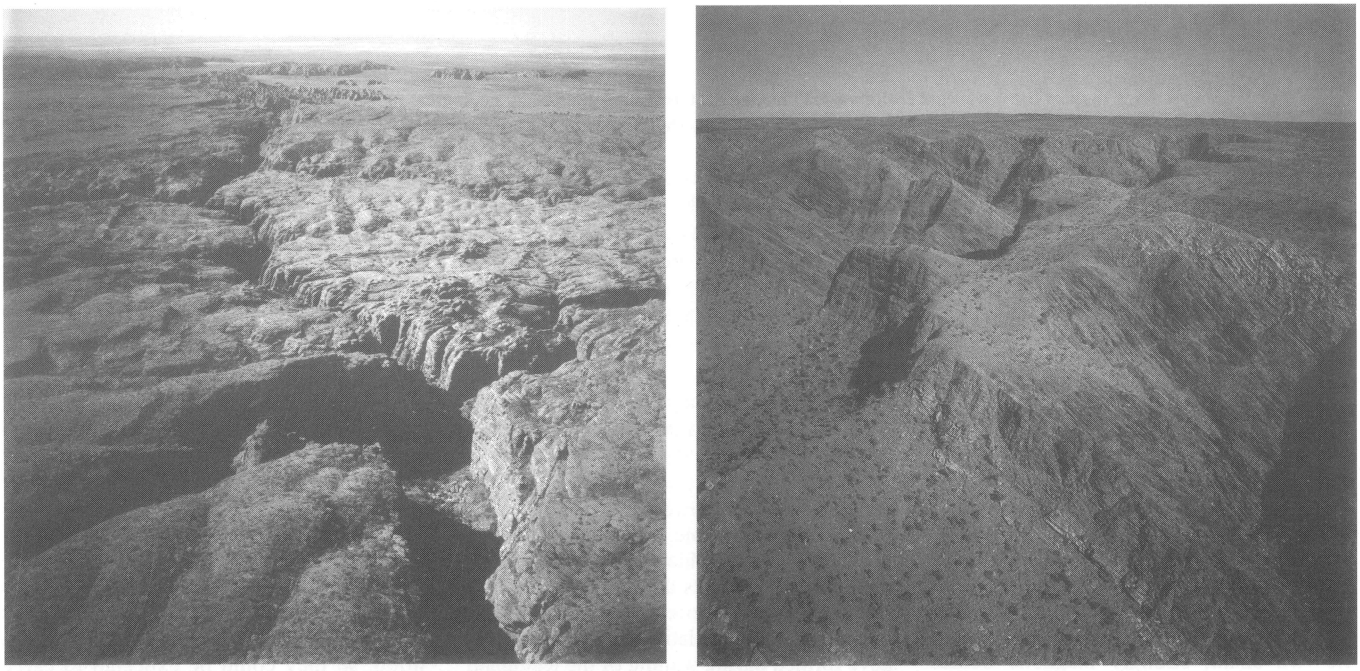

Fig. 4(a) Incised summit plateau of the Bungle Bungle Range, looking SE; (b) bevelled summit of the Osmond Range northwest of Purnululu, showing steeply dipping Proterozoic sandstone truncated by the ancient (Early Miocene) land surface. Photographs by Ian Oswald-Jacobs.

The summit area of the Bungle Bungle Range is a gently undulating plateau, the remnant of an ancient mature land surface which has been incised by creeks of the present-day Ord River drainage system (Fig. 4a). The incision has led to the development of the deep gorges and clusters of steep-sided beehive-shaped hills that characterise the range, and the high cliffs along its western and northwestern sides. These landforms have been carved out of flat-lying to moderately dipping sandstone and conglomerate of the Devonian Mahony Group, the youngest rocks preserved in the Palaeozoic Ord Basin. The Mahony Group was covered by an unknown thickness, probably several kilometres, of younger Palaeozoic rocks (Mory & Beere 1988: GSWA Bulletin 134) before sedimentation in the Ord Basin ceased with the onset of tectonic activity involving uplift, faulting, local thrusting, and mainly open folding. The Bungle Bungle Range lies within the broad Hardman Syncline, which formed during this tectonism. The tectonism may be correlated with the Alice Springs Orogeny of central Australia 300 Ma ago.

Since then, the Kimberley region appears to have been tectonically stable, apart from some local minor faulting, and has been subjected to subaerial denudation. During this time, vast amounts of rock have been stripped from the region and deposited elsewhere. Units of the Ord Basin succession that overlay Proterozoic rocks to the west and north of the present basin outcrop have been removed by erosion, as has the kilometres-thick sequence of Palaeozoic rocks that was deposited on top of the Mahony Group.

The land surface represented by the summit plateau of the Bungle Bungle Range is the same as that forming the bevelled summits of high ranges nearby — including those along the Osmond (Fig. 4b) and Matsu Ranges to the northwest and north, Mount Ranford and Nicks Bite to the west, and the Albert Edward Range to the southwest — all of which are formed of moderately to steeply dipping Proterozoic sedimentary rocks. The same land surface is also preserved to the south on Dixon Range, which is formed of flat-lying Devonian Mahony Group, like the Bungle Bungle Range (Fig. 4a). The present-day Sturt Plateau, to the south and southeast (Warren 1994: AGSO Research Newsletter 20, 14–16), is part of the same land surface, and shows what the ancient land surface was probably like in the Bungle Bungle Range area before subsequent dissection: a subdued landscape consisting of flat to gently undulating terrain with scattered low residual hills and ridges formed of resistant sandstone. Remnants of this land surface in the East Kimberley — plateaus and bevelled ridge crests — are shown in Figure 5.

To the east of the Bungle Bungle Range, at White Mountain (Fig. 5), the ancient land surface — here formed on Late Cambrian sandstone — is overlapped by the White Mountain Formation. This is a unit of fluvial

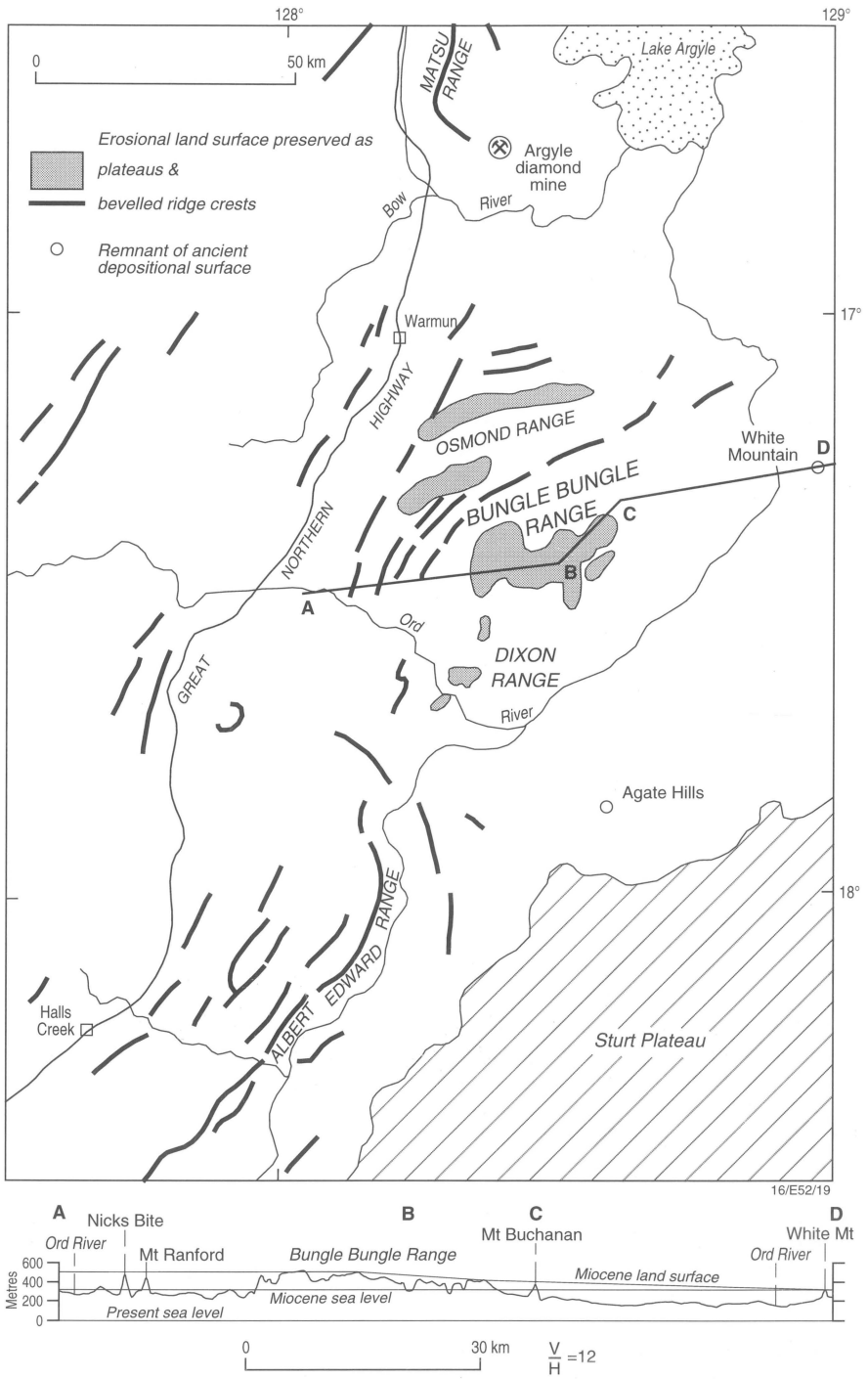

Fig. 5. Remnants of the ancient (Early Miocene) land surface in the Purnululu region of the East Kimberley, and Early Miocene and present-day profiles (along line A–B–C–D).

sandstone and siltstone up to 110 m thick capped by up to 3 m of chert containing non-marine gastropods (*Syrioplanorbis hardmani*) and marine foraminifera (*Ammonia beccarii*) which indicate an age probably no older than Early Miocene (Lloyd 1968; McMichael 1968 — *both* in BMR Bulletin 80) — that is, younger than 23.8 Ma (Jones1995: AGSO Phanerozoic Time Scale 1995). The chert was probably deposited in coastal lagoons at a time when sea level rose during a marine transgression to around 300–350 m higher here than it is now. Sometime after deposition, the White Mountain Formation was tilted to dip 25° to the northeast, along a local fault. Chert about 45 m thick (and 360 m above sea level) that occurs 40 km to the southwest — at Agate Hills, where it overlies Cambrian basalt (Antrim Plateau Volcanics) and limestone (Headleys Limestone) — may also be part of this formation (Mory & Beere 1988: op.cit.).

After the deposition of the White Mountain Formation, a relative lowering of sea level by more than 300 m resulted in a new phase of erosion. The Ord River and its tributaries cut down into the old land surface, eventually to form the present-day landscape. The onset of

renewed erosion on land probably coincided with a sudden increase in sedimentation at the beginning of the Miocene offshore in the Joseph Bonaparte Gulf, where sedimentation rates have remained high to the present day (Petrel Sub-basin stratigraphic chart 1996: AGSO). The spectacular landforms of the Bungle Bungle Range are the results of this Miocene to Recent erosion, as are most of the steep-sided ridges and plateaus in the Kimberley region. A profile of the land surface immediately before incision, the sea level at that time, a profile of the present-day land surface, and the present-day sea level are shown in Figure 5.

The amount of erosion that has taken place in the Purnululu National Park of the East Kimberley during the last 23.8 Ma is comparable to that in the Warrumbungles National Park of New South Wales, where the erosional remnants of a large central volcano that was active 19 Ma ago provide another — although very different — scenic attraction (Duggan & Knutson 1993: 'The Warrumbungle volcano'; AGSO booklet).

An economically important effect of the latest erosional phase, following deposition of the White Mountain Formation, may be the uncovering of the Argyle diamond pipe and the subsequent deposition of diamond-bearing alluvial sediments downstream. The diamond pipe crops out in a small valley at an elevation more than 200 m lower than the old land surface represented by the bevelled top of the nearby Matsu Range. The pipe, which consists of two or more volcanic vents filled with pyroclastics similar in age to country rocks alongside (Boxer & Jaques, 1990: Australasian Institute of Mining & Metallurgy, Monograph 14, 697–706), may not have been exposed before the Miocene. The alluvial gold deposits currently being worked in the Halls Creek area to the south-west of the Bungle Bungle Range also post-date the White Mountain Formation.

How ancient is the Bungle Bungle Range? Being a result of erosion that has taken place in the East Kimberley since the Early Miocene, the range, like most other ranges in the region, is no more than 23.8 Ma old.

[1] AGSO Division of Regional Geology & Minerals, GPO Box 378, Canberra, ACT 2601; tel. +61 6 249 9667, fax +61 6 249 9983.

The Mount Isa geodynamic transect

The deep seismic reflection profile south of Mount Isa and Cloncurry

Bruce Goleby[1], Barry Drummond[1], & Tyler MacCready[2]

Interpretations of the deep seismic reflection and geological mapping data acquired along the Mount Isa geodynamic transect have contributed to the development of a new crustal-scale depth section of the Mount Isa Inlier. Key features of the section include a transitional crust–mantle boundary, a marked difference in the structure of the top 5–10 km between the Eastern Fold Belt and the Western Fold Belt, and the imaging of several major fault systems that cut through the crust. The structure imaged in the Eastern Fold Belt appears to reflect east–west shortening that developed after an episode of rifting (Lake Mary Kathleen Zone). West-vergent thrusting and folding continued across the Pilgrim Fault and into the Kalkadoon–Leichhardt Belt, but in the Leichhardt River Fault Trough (Western Fold Belt) the sense of structuring flipped to east-vergent. The Mount Isa Fault system and the associated lithological sequences now all dip to the west.

The Australian Geodynamics Cooperative Research Centre (AGCRC) undertook the Mount Isa geodynamic transect as part of a multidisciplinary study of the structure and evolution of the Mount Isa Inlier. This transect is one of several AGCRC projects designed to provide a geodynamic synthesis of the inlier. Its objective is to map the depth extent and internal form of the structures and geological blocks in the inlier, which in turn will improve our understanding of mineralisation at the local scale by placing it in a regional three-dimensional context.

AGCRC conducted a series of field experiments designed to define the crustal structure of the inlier — primarily its boundaries and the geometry of its major domain boundary faults; and secondarily, the geometry of internal features of its tectonic units, and the form of its granite intrusions. On the regional scale, the crustal structure beneath the Mount Isa Inlier will be compared with the crustal structure of the crust to the east and west of the inlier. Understanding these features will provide constraints on the relative importance of compressional thrusting and folding, extensional tectonics and basin formation, and strike-slip and transform faulting during the evolution of the inlier.

A wide range of geological, geochemical, and geophysical studies supported the transect, which comprised two seismic reflection traverses (Fig. 6): one oriented east–west and 255 km long; the other subparallel and 30 km long in the Wonga Belt north of Duchess. The main traverse, about 20 km south of the townships of both Mount Isa and Cloncurry, extends through a region of excellent outcrop and covered by numerous detailed maps. The Duchess traverse crossed both the Pilgrim Fault and the Fountain Range Fault.

To provide constraints on the crustal structure, a seismic crustal-refraction survey 500 km long was carried out along the full length of the reflection profile (Fig. 6). Complementary seismic work — including low-fold 3D reflection surveys, a tomographic survey, and high-resolution refraction surveys — was undertaken over several important structures to improve our understanding of them. Potential-field studies along the seismic traverses included the acquisition of detailed gravity, ground magnetic, susceptibility, and radiometric data. Magnetotelluric and SIROTEM soundings were made at several key sites. Detailed geological, structural, and metamorphic mapping was undertaken along the transect, including the logging of seismic shot-hole cuttings. Regolith data were recorded both from the seismic shot-holes and the surrounding area. Bottom-hole samples from the shot-holes were taken for whole-rock and trace-element geochemical analyses, and selected samples were used for fission-track analysis.

This wealth of new data, primarily coming from depth sections, and the vast amounts of existing Mount Isa data have necessitated the development of better visualisation methodologies. The new data have been built into a Mount Isa geodynamic transect GIS, which uses, as its base, the early AGSO Mount Isa Mineral Province 1:500 000 GIS (Jagodzinski et al. 1993: AGSO Metallogenic Atlas Series 1, Vol. 1). The transect GIS is the subject of a companion paper (Wyborn et al., p. 10 of this issue).

Large-scale crustal structure

The seismic refraction results indicate that the crust is thick throughout the region. The crust–mantle boundary is not sharp but is a thick (up to 15 km) transitional zone. The most interesting feature is the presence of a high-velocity (7km s^{-1}) lens-shaped body in

the middle crust. The large-scale crustal structure is discussed further in a companion paper (Goncharov et al., p. 9 of this issue).

Detailed upper crustal structure

The seismic reflection has revealed the nature and geometry of several of the major domain boundary faults, including the Cloncurry Fault, the Quilalar Fault, and the Mount Isa Fault. Some are reflective, but others are interpreted from the truncation of reflections from the sedimentary or volcanic sections. The Cloncurry Fault is imaged as an east-dipping series of weak reflections that apparently sole at about 7 km. The Mount Isa Fault appears to be part of a family of faults that dip west at 70° (Fig. 7). One of these, the Adelheid Fault, is a highly reflective zone that projects downwards from the surface and extends westwards beneath the Sybella Granite. Its pronounced reflectivity might be a product of hydrothermal alteration. The Sybella Granite is imaged as a moderately thin body intruded subparallel to the stratigraphy.

The May Downs Fault, Pilgrim Fault, and Fountain Range Fault are interpreted to be near-vertical strike-slip faults within the upper crust. The Pilgrim and Fountain Range Faults, which appear to link at depth, seem to be part of a strike-slip system that involved at least the upper half of the crust and would account for the mapped strike-slip motion along these faults without major vertical displacement of the juxtaposed sections. The May Downs Fault is interpreted to be subvertical at depth according to the strong discontinuity of reflections in the subsurface.

The crustal structure inferred from the seismic data within the Eastern Fold Belt is markedly different from that imaged within the Western Fold Belt. The Eastern Fold Belt evinces a series of easterly dipping features which in places sole onto or cut a highly reflective, gently east-dipping reflective zone that lies beneath almost the entire Eastern Fold Belt (Fig. 8). This presumably older, gently dipping reflective zone is interpreted as a major regional detachment surface. Huang (1994: Australian Crustal Research Centre, Monash University, Technical Publication 21) mapped this surface as a thrust east of the Pilgrim Fault near the Roos Mine Thrust, and interpreted it as the western edge of the Mitakoodi Fold Belt.

Within the Marimo basin (in the Quamby–Malbon Zone), the seismic recordings have imaged a zone of prominent east-dipping reflectors that are interpreted as a major fault or shear zone. Although there is no major offset mapped at the surface, we infer that its reflectivity is due to hydrothermal alteration. This inference is supported by the nearby Mount McNamara Cu–Au mine, where an east-dipping zone of alteration 200 m wide has been mapped.

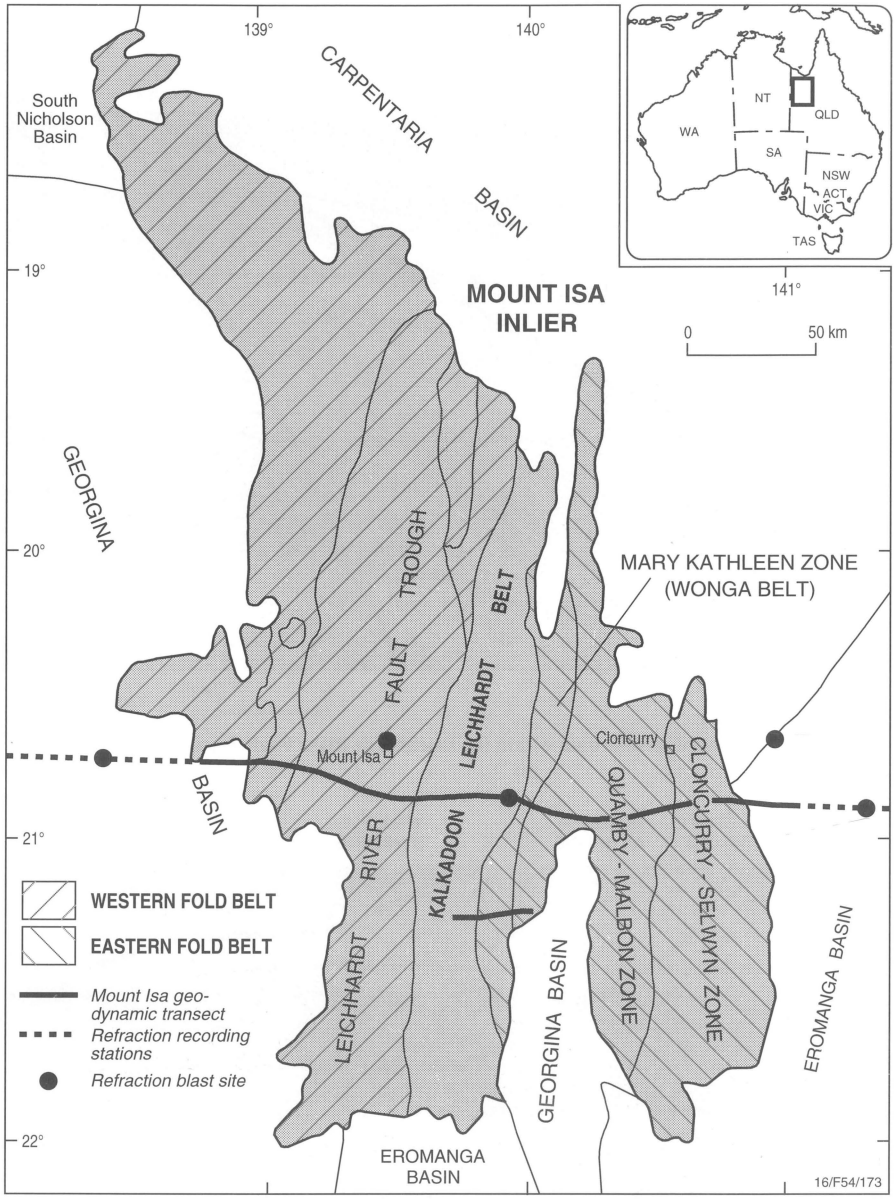

Fig. 6. Tectonic provinces of the Mount Isa Inlier, and locations of both the crustal refraction profile and the deep seismic reflection traverses (components of the Mount Isa geodynamic transect).

In the Mary Kathleen Zone, the seismic data distinguish a prominent linear reflective zone that correlates with a major west-vergent thrust at the western rift margin of the Eastern Fold Belt (Blake 1992: in AGSO Bulletin 243, 181–190), and therefore is interpreted as a fundamental early rift boundary. The Wonga Belt, although not imaged in detail, extends to depth, and appears to link into a much more gently west-dipping reflective zone about 5 km down.

By contrast with the Eastern Fold Belt, the faults imaged by the seismic data in the Western Fold Belt are reminiscent of thick-skinned tectonics. These faults dip easterly in the Kalkadoon–Leichhardt Belt, and westerly in the Leichhardt River Fault Trough. There is no evidence of any major gently dipping structures in the Kalkadoon–Leichhardt and Western Fold Belts (Fig 7).

[1] AGSO Division of Marine, Petroleum & Sedimentary Resources, GPO Box 378, Canberra, ACT 2601; tel. +61 6 249 9404 (BG), +61 6 249 9381 (BD); fax +61 6 249 9981; e-mail bgoleby@agso.gov.au, bdrummon@agso.gov.au.

[2] Department of Earth Sciences, Monash University, Clayton, Vic. 3168; tel. +61 3 9905 4878; fax +61 3 9905 5062; e-mail tylermac@artemis.earth.monash.edu.au.

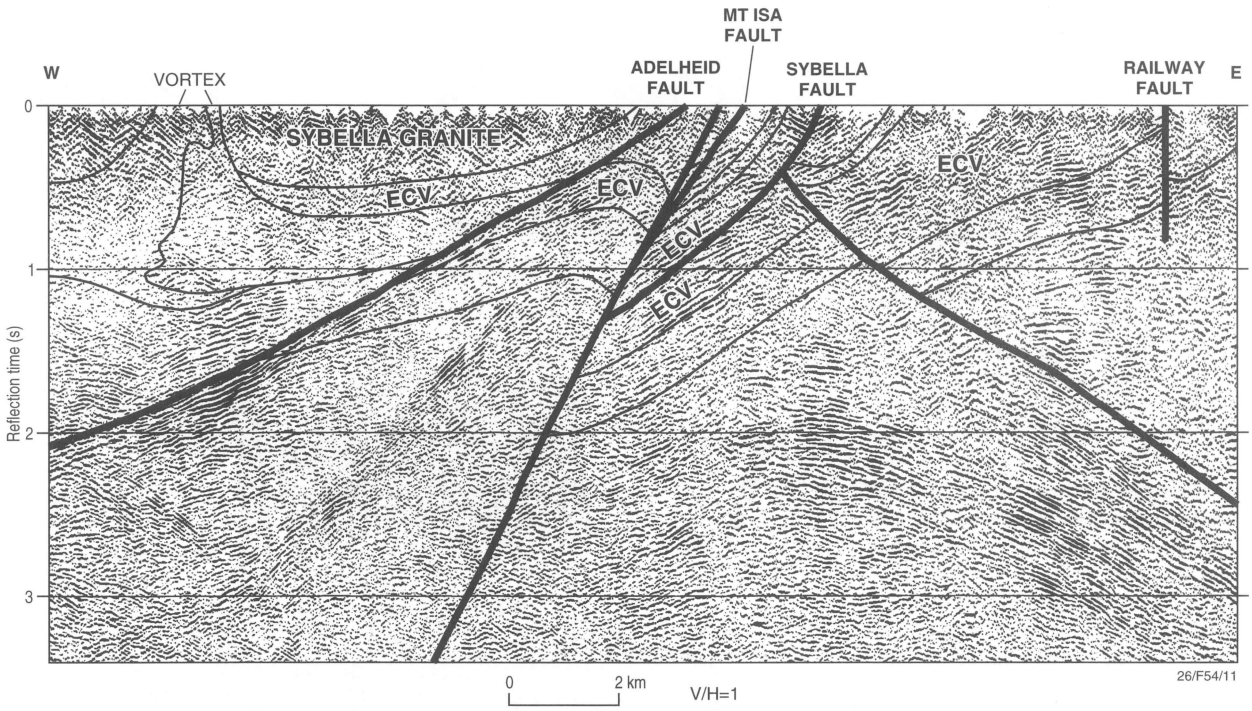

Fig. 7. Portion of seismic data within the Leichhardt River Fault Trough.

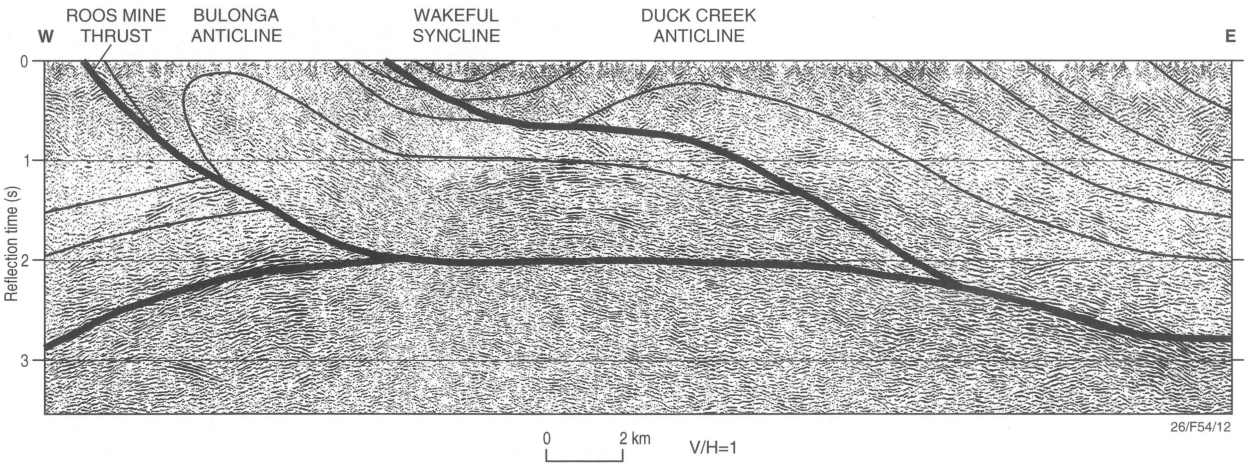

Fig. 8. Portion of seismic data within the Eastern Fold Belt (Mitakoodi Fold Belt).

The Mount Isa geodynamic transect
Implications of the seismic refraction model

Alexey Goncharov[1], Clive Collins[1], Bruce Goleby[1], Barry Drummond[1], & Tyler MacCready[2]

Refraction/wide-angle seismic data recorded along the Mount Isa seismic transect by the Australian Geodynamics Cooperative Research Centre in 1994 (Goleby et al., p. 6 in this issue) evince considerable lateral variation in velocity (Fig. 9). Low-velocity layers are common in the crust and in the crust–mantle transition zone, and lateral variations in velocity are apparent in the upper 15 km of the crust. In the Western Fold Belt, velocities are typically 5.7–6.1 km s^{-1}; Fig. 9). As the Western Fold Belt's integrity is disturbed by wide and numerous north–south-oriented faults and fault zones, such as the Mount Isa Fault, these low velocities, west of the Pilgrim Fault, might be a consequence of the major influence of fault zones on the physical parameters along this part of the transect. By comparison, velocities of 6.1 km s^{-1} and higher typically prevail in the upper 15 km of the Eastern Fold Belt crust, which looks more consolidated. The most intriguing feature of the velocity model is a mid-crustal high-velocity (>7 km s^{-1}) body in the centre of the line.

Seismic refraction profiling estimates the distribution of rock types at depths in the crust by measuring the velocity at which seismic waves travel in the various rock units. One way to explore what the velocity image (Fig. 9) means in geological terms is to look at similar seismic models in other parts of the world. To simplify this comparative analysis, we represent the velocity distribution along the Mount Isa refraction line by two average models (Fig.10). The first is the whole-line average, and the second is an average for the middle anomalous part of the line in the distance range 230–320 km (Fig. 9). These models are similar, except for the high-velocity anomaly in the middle crust.

Comparisons of the Mount Isa velocity model with those of other Australian Proterozoic or Archaean regions indicate no similar mid-crustal anomalies for these regions. Velocities higher than 7 km s^{-1} at depths less than 20 km have never been reported in Australia, for which the middle part of the Mount Isa Inlier is unique. However, it is not only the high-velocity anomaly in the middle crust which distinguishes the velocity model for the Mount Isa region from those of other Precambrian regions in Australia. The background velocity values in the depth range 25–45 km in the Mount Isa region are systematically lower than those in other Australian Proterozoic and Archaean average models. Similar differences are apparent between the Mount Isa and global average seismic velocities, and between the Mount Isa and world average models for shields and platforms. These poor correlations indicate that the anomaly at Mount Isa is unusual for Precambrian crust and is probably the result of a specific geological process, whose age is not well constrained at this stage.

If we examine seismic models for extended and rifted continental crust, the high velocities in the middle crust of the Mount Isa Inlier are not so unusual. Velocities up to 6.85 km s^{-1} detected in the Lake Superior and Lake Michigan mid-continental rift system in Canada at a depth of 10 km (Luetgert & Meyer: 1982: Geological Society of America, Memoir 156, 245–255) were interpreted to remain at least as high down to the Moho at the average depth of 45 km.

An even closer similarity can be seen between Mount Isa velocity models and those of oceanic and continent–ocean transitional regions (Fig. 10). Models of oceanic and rifted continental crust which we have chosen for comparison are simplified models from the US Atlantic margin (Holbrook et al. 1994: Journal of Geophysical Research, 99, B5, 9155–9178). These are limited to basement velocities because we do not discuss the velocities in sedimentary rocks here. Regional extension is normally associated with increased heat flow, thinning of the crust, and the creation of weakened zones along which melted high-velocity rocks from the lower crust or upper mantle might have been emplaced at a higher level in the crust as part of an underplating process.

The Early to Middle Proterozoic tectonic history of the Mount Isa region indicates that numerous ensialic rifting events preceded the Isan Orogeny (between 1620 Ma and 1500 Ma). Most of these events are associated with bimodal volcanism, and some of the rifting might have been close to creating new oceanic crust. Crustal shortening during the Isan Orogeny thickened the previously thinned crust back to high continental values of about 55 km. This shortening of the Mount Isa crust might have resulted in subduction, of which the consistently westward-dipping high-velocity layer is the palaeosubduction zone. However, we lack information about the continuity of the velocity structure in the north–south direction, and as yet we cannot determine if the apparently isolated high-velocity body in the middle crust is connected to the lower crust to the north or south. Also, the products of the Isan Orogeny exclude the basic features that typify the subduction process (high-pressure metamorphism, magmatic arcs, obducted ophiolites), and at this stage we consider subduction of oceanic crust to be an unlikely explanation for the velocity structure of the region.

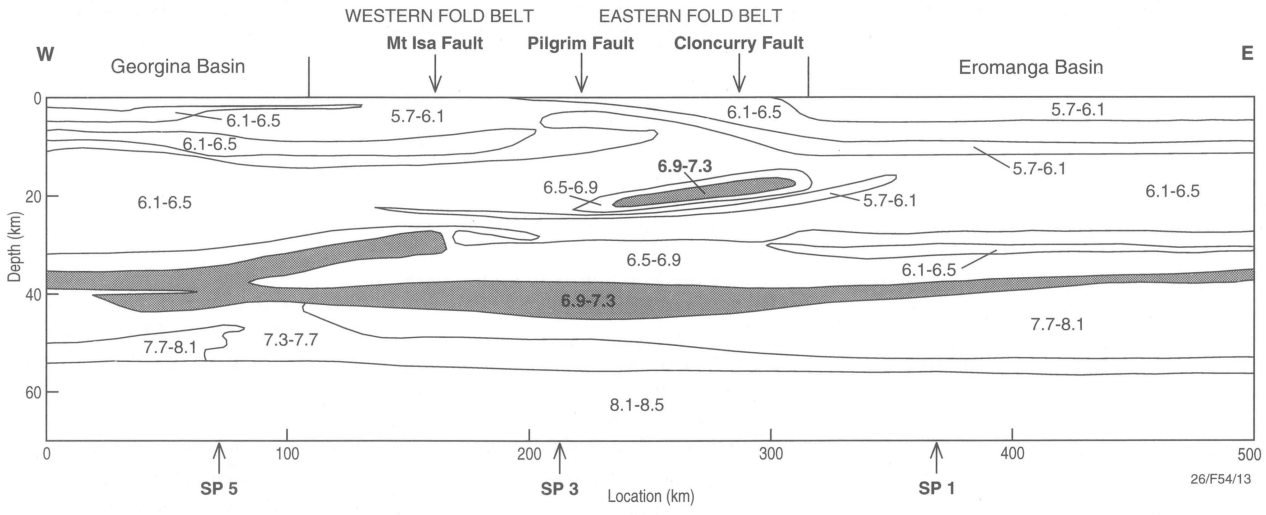

Fig. 9. Seismic velocity distribution along the Mount Isa geodynamic transect.

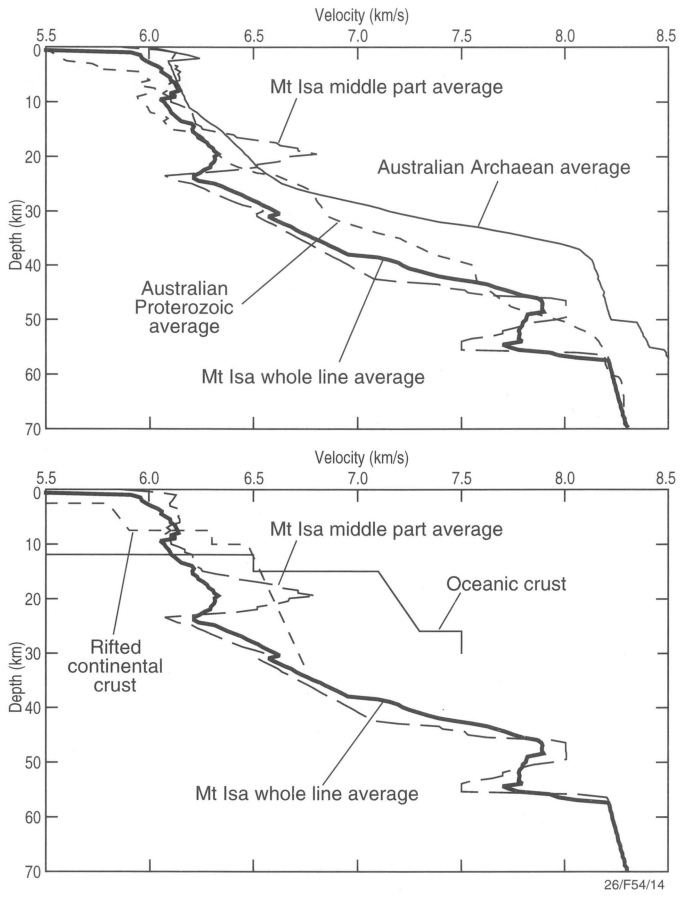

Fig. 10. Mount Isa velocity models in the global context.

We have to conclude that there are several possible options to explain when and how high-velocity material was emplaced at a mid-crustal level, and what it means in terms of rock composition. The emplacement options can be divided into two groups: magmatic and tectonic (structural). The apparent linearity of the bounding edges of the high-velocity anomaly suggests that it is structurally controlled. However, models of magmatic emplacement are easier to reconcile with the way the high-velocity rock is confined by a generally low-velocity crust. In order to resolve these issues, the refraction and wide-angle seismic results from the Mount Isa transect are being applied to investigate the relationship between refraction velocities and the petrology of middle and lower continental crust. The outcome will help to explain both the low-velocity background in the depth range 25–45 km and the low-velocity zones in the top 15 km of the crust, particularly in the Western Fold Belt.

[1] AGSO Division of Marine, Petroleum & Sedimentary Resources, GPO Box 378, Canberra, ACT 2601; tel. +61 6 249 9595 (AG), +61 6 249 9544 (CC), +61 6 249 9404 (BG), +61 6 249 9381 (BD); fax +61 6 249 9981; e-mail agonchar@agso.gov.au, ccollins@agso.gov.au, bgoleby@agso.gov.au, bdrummon@agso.gov.au.

[2] Department of Earth Sciences, Monash University, Clayton, Vic. 3168; tel. +61 3 9905 4878; fax +61 3 9905 5062; e-mail tylermac@artemis.earth.monash.edu.au.

The Mount Isa geodynamic transect

A 2.5-dimensional metallogenic GIS analysis

Lesley Wyborn[1], Bruce Goleby[2], Barry Drummond[2], & Robyn Gallagher[3]

Predicting the third dimension in geographic information systems (GIS) is becoming increasingly critical to metallogenic analysis. Most geological GIS packages so far completed are essentially 2-dimensional (2D) visualisations of the many forms of geoscientific data sets. However, developing truly predictive 3D geoscientific GISs in regions where a network of subsurface data is not available is a challenge, as many aspects of geoscientific data are extremely variable and rarely form mathematically predicable patterns in the subsurface — particularly in regions of complex folding and faulting such as Mount Isa. An ideal opportunity to attempt to develop techniques for a GIS-based 3D metallogenic analysis was provided by the availability of digital data from three sources:

- **the Mount Isa geodynamic transect, undertaken by the Australian Geodynamics Cooperative Research Centre (AGCRC; Goleby et al., p. 6 of this issue; Goncharov et al., p. 9 of this issue);**
- **the Mount Isa 1:500 000 GIS package of maps (Wyborn et al. 1993: 'Mount Isa digital GIS package', AGSO); and**
- **the Mount Isa 1:250 000 geological transect map (Blake & Stewart 1992: 'Geology of the Mount Isa–Cloncurry transect', BMR–AGSO).**

Our initial approach was to integrate the vertical dimension of the seismic data with 2D maps and images into a simple 2.5D model as a precursor to a 3D GIS analysis, which is continuing at AGSO. Our specific goal was to determine which faults and, if possible, which types of faults were more important in controlling the various styles of mineralisation in the Mount Isa Inlier.

Preparation of data sets

Although all data sets are available digitally, several modifications were needed to ensure their effective integration in a 2.5D GIS. Most importantly, the geodynamic transect had to be converted from a non-linear trace onto a straight east–west-trending line along which the planar and vertical sections were to be integrated. As the primary aim was to assess which faults depicted on the transect map were the more important ones in the subsurface, each individual fault had to be uniquely coded so that all arcs representing each distinct fault could be selected simultaneously. Names of faults that were stored as cartographic annotations also had to be converted to searchable attributes. Although the seismic interpretation and the digital geological maps were developed at different times, all geological attributes from the different geological maps and seismic sections also had to be coded identically.

Integration and processing of data sets

To effectively integrate the geological interpretation of the seismic reflection data and the geological maps, the 2D maps were bilinearly transformed (i.e., 'tilted') to give an impression of the top surface of a cube. These plans were then split along the average northing of the main seismic traverse (Goleby et al. op. cit.) to give a northern and a southern plan. The top of the seismic (depth) data and resultant interpretations were then matched to the southern edge of the northern plan. This enabled clear visualisation of connections between the faults in the plan view and those imaged in the seismic reflection section (Fig. 11).

Metallogenic analysis

The main aim of the Mount Isa 2.5D analysis was to determine which of the faults previously mapped at the surface penetrate the deeper crustal levels as imaged in the geodynamic transect data. An earlier seismic transect in the Eastern Goldfields province of the Yilgarn Craton had shown that the more metallogenically important faults at the surface were those that appeared to penetrate the middle crust as imaged in the seismic data (Goleby et al. 1993: BMR Record 1993/54, 85–90). In the Mount Isa data sets, an attempt was made to match each major fault imaged in the seismic data with faults portrayed on the surface geological maps. Buffers were developed along each surface fault and then intersected with the mineral deposit database (Raymond 1992: BMR, Mineral Resources Report 11), to determine which faults are associated with significant mineral deposits, and what the distribution of the various commodities is along each fault.

Metallogenic results

The most important result from the 2.5D analysis is that most of the major structures that are both associated with mineral deposits and visible in the seismic data are *inclined* and terminate in mid-crust. In contrast, the major vertical structures imaged in

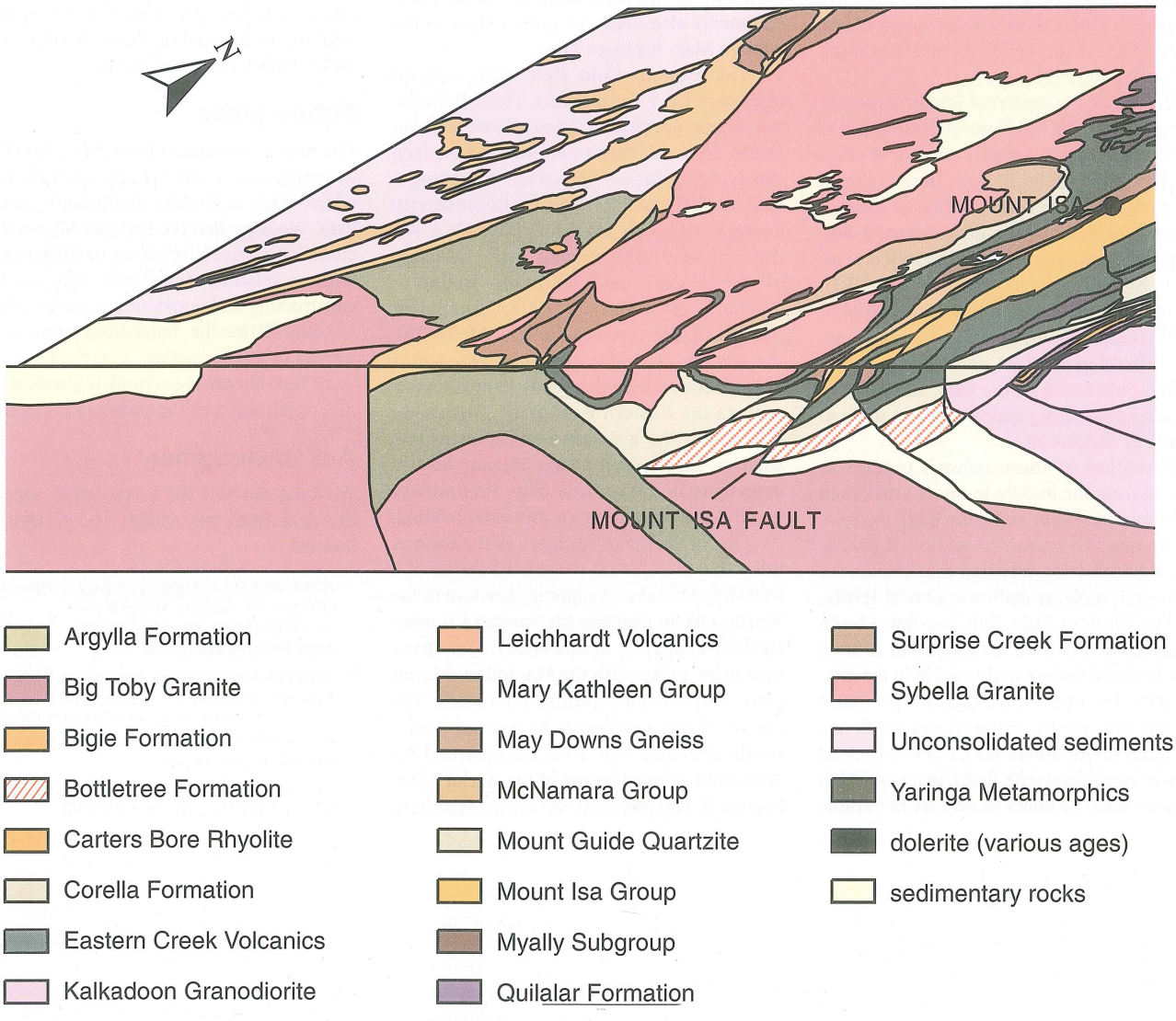

Fig. 11. Part of the 2.5D model of the Mount Isa–Cloncurry region. The top surface shows the regional geology; the front section shows the seismic interpretation. This visualisation shows clear connections between faults in the plan view and those imaged in the seismic section.

the seismic data — such as the Pilgrim, Termite Range, and May Downs Faults — do not host any large mineral deposits, even though they appear to penetrate to the middle crust. This could imply that major movement on these vertical structures postdated any significant hydrothermal activity; indeed, these faults might relate to Palaeozoic and younger events.

From the seismic data, the Mount Isa Fault, which is immediately adjacent to the major Mount Isa, Hilton, and George Fisher Pb–Zn deposits and the Mount Isa Cu orebody, is a major west-dipping structure connecting to mid-crustal levels. It is tempting to assert that this major structure facilitated movement of deep-seated ore-bearing magmatic or metamorphic fluids from the middle crust. However, the Pb-isotope data from the Pb–Zn ore show no evidence of fluids derived from a pre-existing granulite basement older than 2000 Ma, nor is there any evidence of fluids related to the ~1500 Ma magmatic and metamorphic events at Mount Isa. Instead the Pb-isotope data support a synsedimentary origin for the Mount Isa Pb–Zn deposit, and indicate that the Pb-isotope composition of this ore system is compatible with that of the surrounding host rocks (Sun et al. 1994: AGSO Research Newsletter 20, 1–2).

Similarly, the preferred interpretation of the stable-isotope and fluid-inclusion data is that the fluids that formed the world-class Mount Isa Cu orebody were derived from low-grade metamorphic fluids or basinal brines, rather than from deep-seated metamorphic or magmatic fluids (Heinrich et al. 1995: Economic Geology, 90, 705–730). West-dipping splays from the eastern side of the Mount Isa Fault, portrayed by the seismic reflection data as connecting to the lower-grade areas to the east, might have provided connecting pathways from there to the site of deposition.

If neither of these deposit types was derived from the middle to lower crust, then the Mount Isa Fault, as portrayed in the seismic images, might have functioned primarily as an effective focusing mechanism for fluids derived from shallower crustal levels.

The Western Fold Belt has few Pb–Zn deposits, of which all are large and located close to major faults clearly visible in the seismic data. In contrast, Cu deposits are more prolific and mostly insignificant (with the exception of the Mount Isa Cu orebody), and occur in association with faults, many of which are assumed to be minor as they are not visible in the seismic data. If the Pb–Zn and Cu moved as part of the one fluid system during the major D2 and D3 metamorphic event at around 1530 Ma (Perkins et al. in press: Economic Geology), this spatial segregation between the two systems is difficult to explain. Uranium and Cu deposits have a much closer spatial association in the Western Fold Belt (see Heinrich et al.: op. cit.) than there is between Pb–Zn and Cu. This observation is compatible with the geochemical and isotopic evidence indicating that the major movement of Pb–Zn occurred during basin-forming processes at around 1650 Ma (Sun et al., p. 20 of this issue), whereas the distribution of Cu and U was controlled by metamorphic and deformational processes at around 1530 Ma.

The older Kalkadoon–Leichhardt Belt, in the central part of the Mount Isa Inlier, shows no seismic evidence of major structures which could be related to an earlier continental-margin system (e.g., Wilson 1978: Precambrian Research, 7, 205–235), nor does it show any evidence of a mid-crustal subhorizontal structure. In contrast to the Western and Eastern Fold Belts, there are also no major deposits hosted within this older basement block. These comments also apply to some extent to the western Mary Kathleen Zone.

The Eastern Fold Belt hosts several important Cu ± Au deposits. Here, the seismic image portrays a series of east-dipping faults, all connected to a more major deep flat-lying surface — possibly indicating a path to facilitate fluid flow. Interestingly enough, although many of these Cu ± Au deposits have been related to the intrusion of the Naraku and Williams Batholith (Wyborn & Heinrich 1993: Australian Institute of Geoscientists, Bulletin 13, 27–30), the seismic data did not show any major deep plutons where the geodynamic transect crosses the Eastern Fold Belt. This could reflect that the granites were emplaced as shallow sheets, and hence are not readily detectable in the seismic data. Preliminary gravity modelling supports this interpretation.

One of the major surprises of the seismic reflection profile was the identification of a substantial blind east-dipping structure in the Marimo basin near the McNamara Cu mine (Goleby et al., p. 6 of this issue). This structure is on strike with the Hampden, Mount Dore, and Selwyn deposits to the south. The control of these orebodies by a major north–south structure was first documented by AGGSNA (annual report of the Aerial, Geological & Geophysical Survey of Northern Australia for the period ending 31st December 1936), which noted that these deposits are associated with a zone of shearing passing though Kuridala, Mount Elliott, and the area west of Mount Cobalt. AGGSNA suggested that there is further potential along this zone and to the north and south of it.

Conclusions

This preliminary 2.5D assessment has highlighted the connection between the larger deposits in the Mount Isa Inlier and the more significant faults as imaged by the seismic data. However, a fault that penetrates to the mid-crust is no guarantee that it will be mineralised; indeed, the major deep vertical fault systems are essentially barren. Faults controlling the large deposits are inclined. Although they penetrate to the mid-crust, independent geochemical and isotopic evidence argues against the sourcing of mineralising fluids from such deep levels. Instead, the fluids appear to have been derived from either sedimentary basinal brines or shallow magmatic and/or low-grade metamorphic processes. The major faults could have provided distributory channels for mineralising fluids derived from these shallower crustal levels.

Future plans

The next development from this 2.5D GIS is to progress to a full 3D approach for areas where there is limited drillhole or seismic data. We hope that the methodology will include interactively selecting profiles in areas with no seismic or drillhole data, and then constructing and constraining cross-sections to better define the major fluid pathways involved in ore formation. The final step will be to link the cross-sections to produce true 3D visualisation of the subsurface geometry.

Acknowledgment

We thank the AGCRC for providing access to the data from the Mount Isa geodynamic transect.

[1] AGSO Division of Regional Geology & Minerals, GPO Box 378, Canberra, ACT 2601; tel. +61 6 249 9489, fax +61 6 249 9986, e-mail lwyborn@agso.gov.au.

[2] AGSO Division of Marine, Petroleum & Sedimentary Resources, GPO Box 378, Canberra, ACT 2601; tel. +61 6 249 9404 (BG), +61 6 249 9381 (BD); fax +61 6 249 9981; e-mail bgoleby@agso.gov.au, bdrummon@agso.gov.au.

[3] GISolutions, GPO Box 2237, Canberra, ACT 2601; tel. +61 6 251 3511, fax +61 6 251 3581.

A major magmatic event during 1050–1080 Ma in central Australia, and an emplacement age for the Giles Complex

Shen-su Sun[1], John W. Sheraton[1], Andrew Y. Glikson[1], & Alastair J. Stewart[1]

The emplacement age of the voluminous mafic–ultramafic intrusions of the Giles Complex, central Australia, has been an outstanding issue requiring assessment by modern isotopic-dating techniques. It has relevance to several questions:

- **how are these intrusions related to the 1200-Ma Musgravian orogenic event?;**
- **are they genetic correlatives of the spatially associated felsic volcanics of the Tollu Group?; and**
- **does the Giles Complex magmatism have correlatives elsewhere in central Australia?**

A well-defined isotopic-age framework is also important for reconstructing the pressure–temperature–time (PTt) history of the metamorphosed country rocks of the Musgrave Block. This study has been conducted as a part of the Musgrave National Geoscience Mapping Accord (NGMA) project.

Field relations of the Giles Complex

The Giles Complex, a set of large layered mafic–utramafic intrusions was emplaced in the western Musgrave Block, central Australia (Fig.12), deep in the crust after an orogenic event involving regional granulite-facies metamorphism, deformation, and the generation of synmetamorphic granites at about 1200 Ma (Gray 1978: Journal of the Geological Society of Australia, 25, 403–414). The time of this orogenic event is confined by the emplacement of the Minno augen gneiss, a synmetamorphic granite dated by the SHRIMP zircon U–Pb method at 1198 ± 6 Ma (Sun & Sheraton 1992: AGSO Research Newsletter, 17, 9–11).

In the Champ de Mars area (Fig. 13), K-feldspar porphyritic granite and rapakivi granite appear to intrude the Giles Complex locally along the southern margin of the Hinckley Range intrusion. The SHRIMP zircon U–Pb age for the emplacement of the

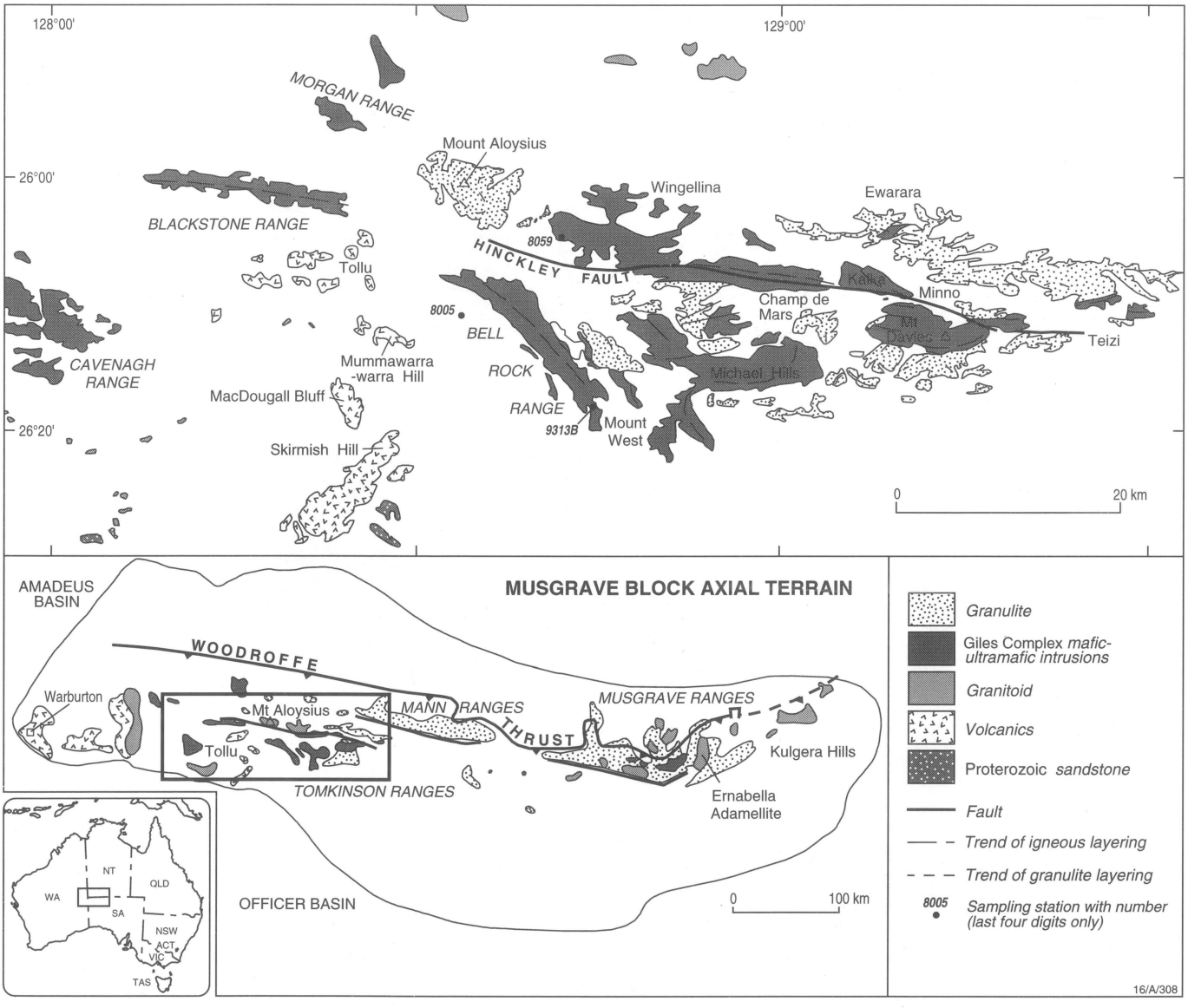

Fig. 12. Field relationships of the Giles Complex, and locations of SHRIMP zircon U–Pb samples.

porphyritic granite is 1188 ± 4 Ma (Sun et al. 1996: 13th Australian Geological Convention, Abstracts, 41, 423). Among the felsic and mafic dykes intruding the Giles Complex, some of the mafic dykes classified as type A show chemical and isotopic similarities to the Giles Complex, indicating that they are likely to be cogenetic. Granophyre within the Bell Rock intrusion (Fig. 12) is interpreted to be a late magmatic differentiate of the enveloping gabbroic intrusion. The zircon U–Pb ages of these and other associated igneous rocks can be used to constrain the time that the Giles Complex was emplaced.

Zircon U–Pb dating by SHRIMP and a magmatic event during 1050–1080 Ma

Zircon U–Pb dating of selected samples was carried out using the SHRIMP 2 at the Research School of Earth Sciences, Australian National University. The results are shown on concordia plots (Fig. 14). A granitic dyke — sample (9198)8059 (Fig. 12) — in the western part of the Hinckley Range gabbronorite intrusion has a $^{207}Pb/^{206}Pb$ age of 1052 ±11 Ma. A rapakivi-textured felsic dyke (91988064; Fig.13) in the southern margin of the Hinckley Range intrusion has a $^{207}Pb/^{206}Pb$ age of 1068 ± 6 Ma; this felsic dyke had been previously supposed to be related to the porphyritic and rapakivi granites dated at 1188 Ma in the Champ de Mars area. A rhyolite sample (91988005; Fig. 12) of the Smoke Hill Volcanics, Tollu Group, has a magmatic $^{207}Pb/^{206}Pb$ age of 1078 ± 5 Ma. A granophyric pegmatite (91989313B; Fig. 12) in the Bell Rock gabbroic intrusion contains large euhedral, simply zoned igneous zircons with a concordant U–Pb age of 1078 ± 3 Ma.

Although a range of emplacement ages for different intrusions of the Giles Complex is possible, we tentatively regard the well-defined age of 1078 ± 3 Ma for granophyre from the Bell Rock gabbroic intrusion as the most probable age of the Giles Complex. This age supersedes the 1200–1185-Ma age bracket previously presented (Sun & Sheraton 1992: op. cit.), and is supported by a preliminary zircon U–Pb age of 1073 ± 5 Ma (from six grains only) for a chilled? phase (or a type A dyke?) of the Hinckley Range gabbronorite intrusion. It is further supported by the study of two leucogabbro samples from the Wingellina Hills intrusion (Fig. 12) emplaced at depths of about 20 km (Ballhaus & Berry 1991: Journal of Petrology, 32, 1–28). These samples yield three-point (clinopyroxene, plagioclase, and whole-rock) Sm–Nd isochrons of 1047 ± 28 and 1077 ± 32 Ma. They contain olivine, and have igneous textures showing only minor recrystallisation, suggesting that metamorphic overprinting is minimal and that the ages reflect emplacement. Our results support an earlier suggestion made by Nesbitt et al. (1970: Geological Society of South Africa, Special Publication 1, 547–564) that felsic volcanics of the Tollu Group and back-intrusion felsic dykes and granophyres associated with the layered intrusions are all genetically related to the Giles Complex.

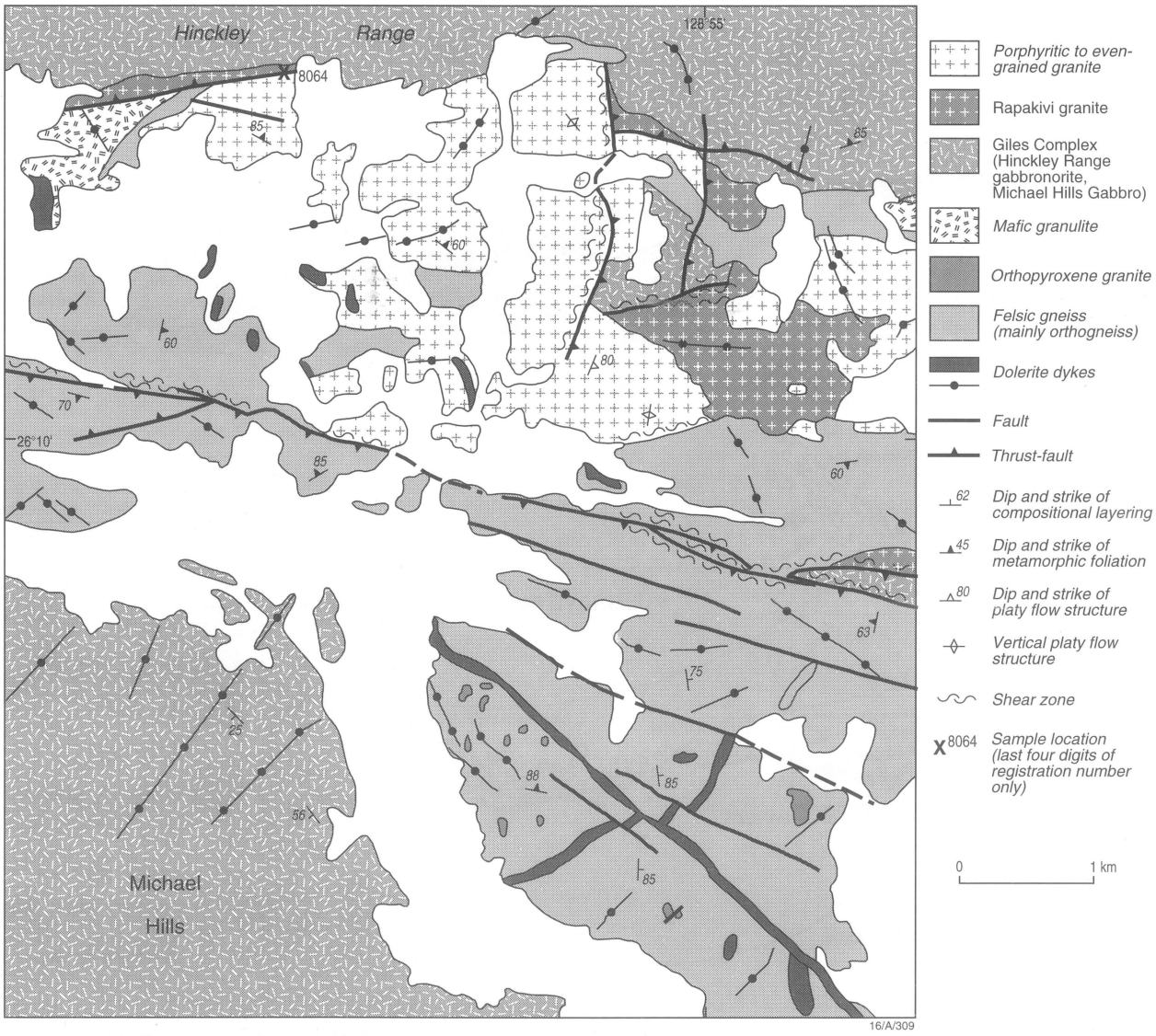

Fig. 13. Field relationships of the Hinckley Range gabbronorite and the porphyritic and rapakivi granites in the Champ de Mars area.

Broader implications

This widespread magmatic event between 1050 and 1080 Ma in the Musgrave Block has profound implications for the second episode of granulite-facies metamorphism, postdating 1200 Ma, described by Clarke et al. (1995: AGSO Journal of Australian Geology & Geophysics, 16, 127–146). It is a major and separate event from the 1200-Ma Musgravian orogeny. Emplacement of a large amount of high-temperature (1200–1300°C) tholeiitic magma into deep crustal levels is believed to have increased the lithostatic pressure and induced granulite-facies metamorphism and crustal melting, resulting in bimodal mafic and felsic volcanic and hypabyssal igneous activity. The range of initial εNd values (+0.9 to –2.5) and the chemistry of 1050–1080-Ma felsic rocks are consistent with magma generation by various processes — including crustal melting of ~1550 and ~1300-Ma felsic granulite-facies country rocks (with εNd of –2.5 to –4.8 at 1070 Ma), and derivation from mafic magmas through extensive crustal assimilation coupled with fractional crystallisation.

The 1050–1080-Ma magmatic event in the western Musgrave Block can be correlated with a similar event more than 400 km to the east in the Kulgera area, eastern Musgrave Block (Fig. 12), and in the Alice Springs area, southern Arunta Inlier. A dolerite dyke swarm in the Kulgera area and the Stuart dyke swarm in the Alice Springs area have been dated by Sm–Nd mineral isochrons (Zhao & McCulloch 1993: Chemical Geology, 109, 341–354) at 1076 ± 33 Ma and 1090 ± 32 Ma, respectively. A period of intraplate lithospheric extension and generation of tholeiitic magma at about 1080 Ma in a wide area covering the Musgrave Block and southern Arunta Inlier is indicated.

[1] AGSO Division of Regional Geology & Minerals, GPO Box 378, Canberra, ACT 2601; tel. +61 6 249 9484 (S-sS), +61 6 249 9384 (JWS), +61 6 249 9591 (AYG), +61 6 249 9666 (AJS), fax +61 6 249 9983.

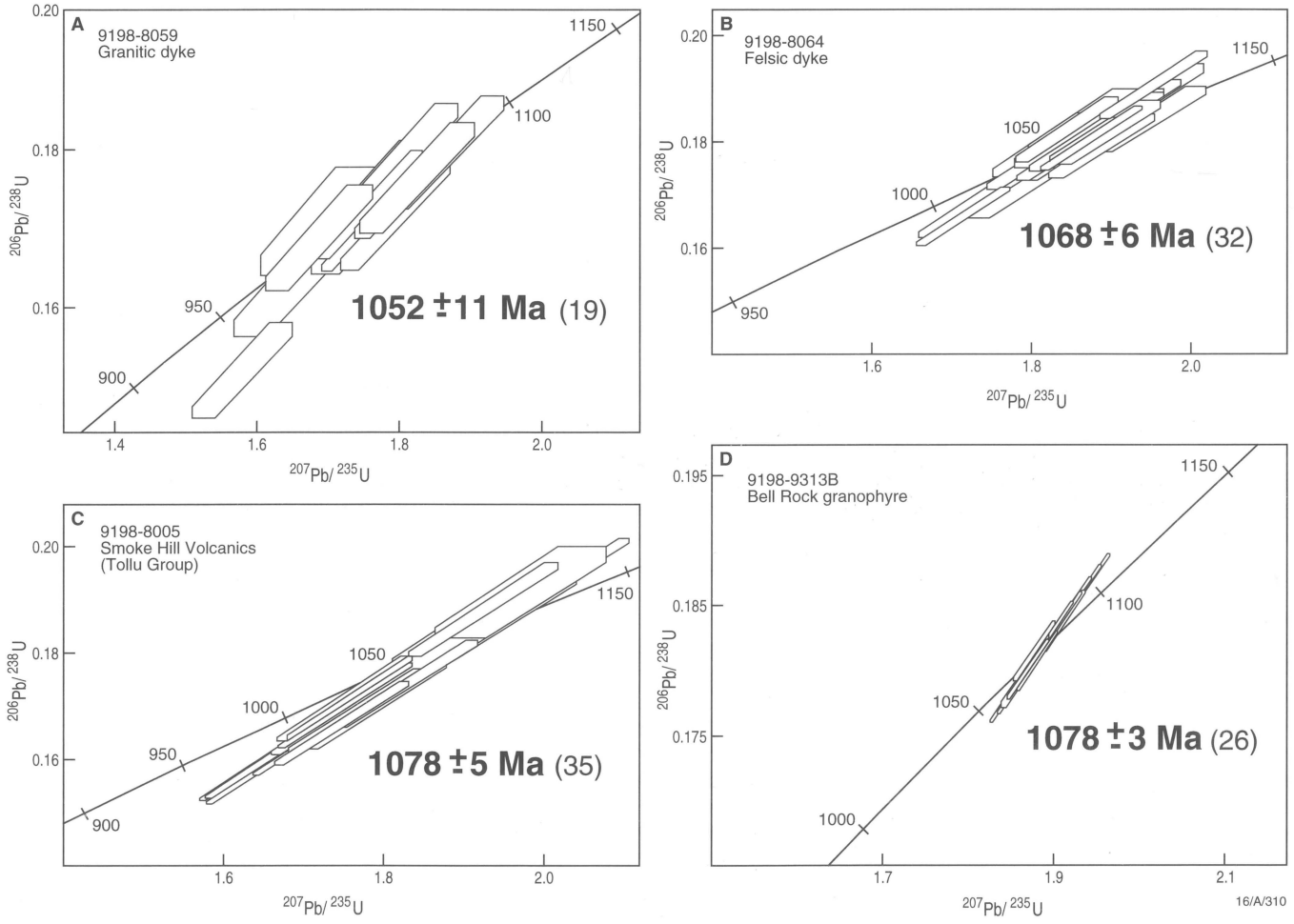

Fig. 14. Concordia plots for samples analysed; the bracketed number to the right of each age refers to the number of SHRIMP spot analyses. (a) A granitic dyke in the western part of the Hinckley Range intrusion. Igneous zircon grains are squat; most are rounded prisms with igneous zoning and inclusions. (b) A rapakivi-textured felsic dyke in the southern margin of the Hinckley Range intrusion. Zircon grains are mostly clear and euhedral, and show variable igneous zoning. (c) A rhyolite sample (91988005) of the Smoke Hill Volcanics, Tollu Group. Igneous zircons are simply zoned. (d) A granophyric pegmatite (91989313B) in the Bell Rock gabbro. Zircon grains are large, euhedral, and simply zoned, and have a very high U content (~ 4000 ppm).

The effective elastic thickness of the Australian crust: a major control on the wavelength and shape of topography and basins

Peter Wellman[1]

Lithospheric strength is an important factor in all large-scale geological processes involving mass transfer, because it controls the wavelength of deformation of the lithosphere and hence the wavelength of the isostatic compensation. The Australian observational evidence is consistent with the lithospheric strength being determined by the thermal age of the lithosphere at the time of loading.

Early theories of the crust, including the Airy and Pratt hypotheses of isostasy, assumed that the lithosphere was moderately weak, and isostatically compensated for crustal loads (such as mountains) directly below them. Later it was appreciated that the lithosphere has a finite strength, so that isostatic compensation of loads is distributed over a broad region below them. The generally accepted model is for the Earth's lithosphere to flex when loaded, as though it is an elastic plate. There is only one parameter controlling the amount and wavelength of flexure; this can be expressed as the effective elastic thickness measured in kilometres.

Karner et al. (1983: Nature, 304, 250–253) discussed a model in which the strength of either continental or oceanic lithosphere is a function of the thermal age of the lithosphere at the time of loading. The effective elastic thickness is controlled by the depth of the 450°C isotherm, such that there is a linear relationship between the log of the time of loading, and the log of the effective elastic thickness. This model is generally accepted for oceanic lithosphere, but not so for continental lithosphere.

Zuber et al (1989: Journal of Geophysical Research, 94, 9353–9367) used the distribution of topography and gravity anomalies in Australia to map the distribution of effective elastic thickness. Each topographic feature imposes a known load on the lithosphere, and the gravity anomalies in the region of the topography show the distribution of the isostatically compensating masses deeper in the lithosphere. In Australia, the effective elastic thickness of the lithosphere varies from 132–134 km over Archaean and Proterozoic crust, to 16–17 km over parts of the Eastern Highlands. Zuber et al. showed that these estimates correlate roughly with the time of lithospheric stabilisation, but they did not discuss the thermal age of the lithosphere at the time of loading.

More recently, Hartley et al. (1996: Earth & Planetary Science Letters, 137, 1–18), discussing lithospheric strength in Africa, have concluded that there is no clear relationship between effective elastic thickness and the thermal age of the continental lithosphere at the time of loading; rather, for Africa, effective elastic thickness depends on the present-day geotherm. The observed Australian data do not correlate with heat flow, because the highest heat flows are in the western Tasman Orogenic Zone and the western part of the Mount Isa Inlier, areas with intermediate values of effective elastic thickness.

The thermal age of the Australian lithosphere is here assumed to correspond to:

- the age of the last major metamorphic and intrusive event in areas of little cover;
- the age of extension where this has led to wide and deep sedimentary basins; and
- the age of formation of new Tasman seafloor for areas of the Eastern Highlands that were upper plate margins.

The age of the topography over most of Australia is taken to be Late Cretaceous, because it must be younger than the extensive mid-Cretaceous marine sediments. In the Eastern Highlands, some uplift is attributed to 80–60-Ma crustal extension, but critically some is caused by underplating associated with Cainozoic volcanism which occurred 30–20 Ma ago in central Queensland and eastern NSW, and 5–0 Ma ago in northeast Queensland and western Victoria. Applying these ages, I find that the thermal age of the lithosphere at the time of loading gives an effective elastic thickness that is the same as that measured to within experimental error.

This result is important for an understanding of geological processes because the strength of the lithosphere is a factor in calculations of deformation due to isostatic effects. The model of Karner et al. should provide the controlling parameter for any lithospheric deformation that does not reset the thermal state of the lithosphere. Examples are crustal deformation by thick-skinned tectonics, depression of the crust due to sedimentation or volcanism, and uplifts due to underplating of the crust, or to isostatic rebound after denudation of topography.

[1] AGSO Division of Regional Geology & Minerals, GPO Box 378, Canberra, ACT 2601; tel.+61 6 249 9653, fax +61 6 249 9983, e-mail pwellman@agso.gov.au.

The precious-metals potential of the Rockley Volcanics in the Lachlan Fold Belt

David A. Wallace[1]

Earlier reports (Wyborn 1988: BMR Research Newsletter 8, 13–14; Wyborn 1990: BMR Research Newsletter 13, 8) highlighted the precious-metal potential of Ordovician shoshonitic magmas in the central Lachlan Fold Belt (Fig. 15). Intrusive complexes and volcanics derived from these magmas host important Cu–Au deposits in the Parkes–Narromine and Orange–Wellington belts, and the Fifield–Nyngan belt contains Alaskan-type mafic–ultramafic intrusions enriched in platinum. These areas are currently the main focus of exploration activity. Following joint AGSO–Geological Survey of New South Wales geological mapping of the Bathurst 1:250 000 Sheet area as part of the National Geoscience Mapping Accord (NGMA; Stuart-Smith & Wallace 1994: Oberon 1:100 000 Sheet, 8830, preliminary-edition geological map, AGSO), a geochemical study of the Rockley Volcanics in the Oberon Sheet area was undertaken. Platinum-group-element (PGE) and Au data from this study form part of this report.

Stratigraphy

The Rockley Volcanics are a series of shoshonitic mafic and ultramafic (peridotite and pyroxenite) extrusive rocks and derived volcanogenic sedimentary rocks emplaced in the Middle to Late Ordovician. They are transitional to and overlie the widespread quartz-rich turbidites of the Adaminaby Group, which was deposited in the Early Ordovician. In the Bathurst 1:250 000 Sheet area south of the Bathurst Granite, they form part of a belt of mafic–ultramafic Ordovician volcanics which correlate with the Sofala Volcanics north of the Bathurst Granite. Elsewhere in the eastern part of the Lachlan Fold Belt, they also correlate with volcanics in the Fifield–Nyngan, Parkes–Narromine, and Orange–Wellington belts, and with the Kiandra Volcanics (Fig. 15).

Geochemistry

The whole-rock chemistry of the Rockley Volcanics is similar to that described by Wyborn (1992: Tectonophysics, 214, 177–192) for Ordovician shoshonites of the eastern Lachlan Fold Belt. Nd-isotope systematics on a basalt sample yielded a εNd value of 5.8, typical of Ordovician shoshonite derived from a long-term light-rare-earth-element- (LREE-) depleted mantle (Wyborn & Sun 1993: AGSO Research Newsletter 19, 13–14). The basalts have high MgO (7–11wt%), high K_2O (1.45–2.52%), and K_2O:Na_2O ratios of 0.4–1.03. The basaltic rocks are also characterised by high large-ion-lithophile-element (LILE) concentrations (Ba up to 5000 ppm) and P_2O_5 (up to 0.31%), and low high-field-strength elements (TiO_2 <0.6%, Nb <10 ppm, Zr <50 ppm, Y <15 ppm) and LREEs (La 3–8 ppm; Ce 6–19 ppm).

Aliquots of selected samples of ultramafic and mafic rocks from the Rockley Volcanics were analysed by fire assay, followed by inductively coupled plasma–mass spectrometry (ICP–MS) for Pt, Pd, and Au, at Analabs in Perth. These samples are a good representation of the variety of Ordovician volcanics throughout the Oberon Sheet area. Three Tertiary basalt samples from the Oberon area were also analysed for PGEs for comparison with the Ordovician volcanics.

The Rockley Volcanics, ranging in composition from peridotite to basalt, have Pt, Pd, and Au abundances similar to Ordovician mafic volcanic suites that Wyborn (1990: op. cit.) described from elsewhere in the Lachlan Fold Belt. [Pt + Pd] abundances range from 5 to 36 ppb, while Au averages 1.5 ppb and has maximum abundances of 3 ppb in mafic volcanics and volcanic-derived sedimentary rocks. These concentrations contrast with the low PGE concentrations in the Tertiary volcanics, in which [Pt + Pd] is <1 ppb. The use of MgO as an index of fractionation (Fig. 16) demonstrates that Pd and Au systematically increase with fractionation, and that Pt abundances increase slightly from peridotite to pyroxenite, then fall appreciably with decreasing MgO; thus, Pt and Pd are inversely related during the pyroxenite–basalt stage of fractionation. Figure 16 suggests additionally that [Pt + Pd] increases with fractionation to a possible maximum ≅20 ppb at MgO ~20 per cent, then levels out as compositions become more basaltic.

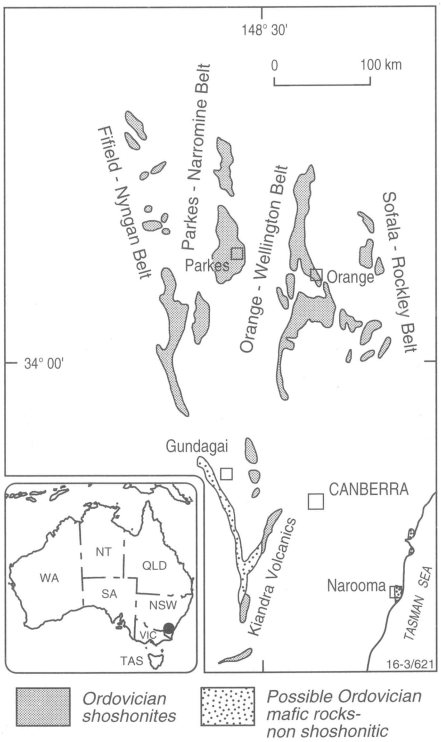

Fig. 15. Locations of Ordovician and possible Ordovician magmatic rocks in the eastern Lachlan Fold Belt.

Pt:Pd:Au ratios derived from interpolated trends in Figure 16 for various rock compositions in the peridotite-to-basalt assemblage are: peridotite (MgO ~35%) 14:5:1; pyroxenite (MgO ~23%) 7:6:1; and basalt (MgO ~8%) 2:5:1. These trends show that the Pd:Au ratio is constant throughout the evolution of the suite, and that there is an overall sevenfold decrease in Pt in the system as it becomes less magnesian. PGE levels and ratios in the volcanolithic samples are consistent with those in the primary magmatic rocks with the same MgO, except for two samples with low Pd (<5 ppb) and Au (<1 ppb) and one sample with high Pt (17.5 ppb) and Pd (19 ppb; Fig. 16). This suggests that the sedimentary and depositional processes which occurred during the history of these rocks had minor significance in mobilising PGE or changing their inherited PGE.

Discussion

The elevated PGE abundances in the Ordovician volcanics in the Oberon Sheet area, and their pattern of variation with fractionation, are consistent with evidence presented by Wyborn (1990: op. cit.) that Ordovician magmas in the eastern Lachlan Fold Belt were sulphur-undersaturated during their early history, and thus retained PGEs in their melts. Pt:Pd:Au ratios of these rocks are also consistent with expected magmatic ratios pertaining to S-undersaturated conditions for Ordovician shoshonites elsewhere in the Lachlan Fold Belt (Wyborn & Sun 1994: AGSO Research Newsletter 21, 7–8). The fractionation history of the mafic–ultramafic rocks suggests that sulphur depletion continued to be a factor in determining PGE concentration throughout the later stages of the evolution of the magmas. In contrast, the consistently low PGE abundances of the

Tertiary basalts provide evidence that these rocks were sulphur-saturated, and that PGEs were removed from their melts at an early stage in the evolution of these magmas.

Although there are analogues for Pt enrichment and high Pt:Pd ratios in the magnesium-rich rocks of Alaskan-type zoned complexes — such as in the Fifield–Nyngan belt, in the Urals, and at Tulameen, Canada (Johan 1994: International Mineralogical Association, 16th General Meeting, Pisa) — there is no clear explanation for the variation in Pt and Pd abundances and lower Pt:Pd ratios in non-cumulate volcanic rocks. Wyborn (1990: op. cit.) reviewed the available experimental evidence to explain the causes of decoupling between Pt and Pd (Amosse et al. 1990: Chemical Geology, 81, 45–53; Johan et al. 1989: Mineralogy & Petrology, 40, 289–309), and concluded that the high partition coefficient of Pt and low coefficent of Pd in the Fe–Pt–Pd alloy system under sustained conditions of high $f(O_2)$ — hence low sulphur fugacity — could be a plausible explanation for the moderately rapid depletion of Pt.

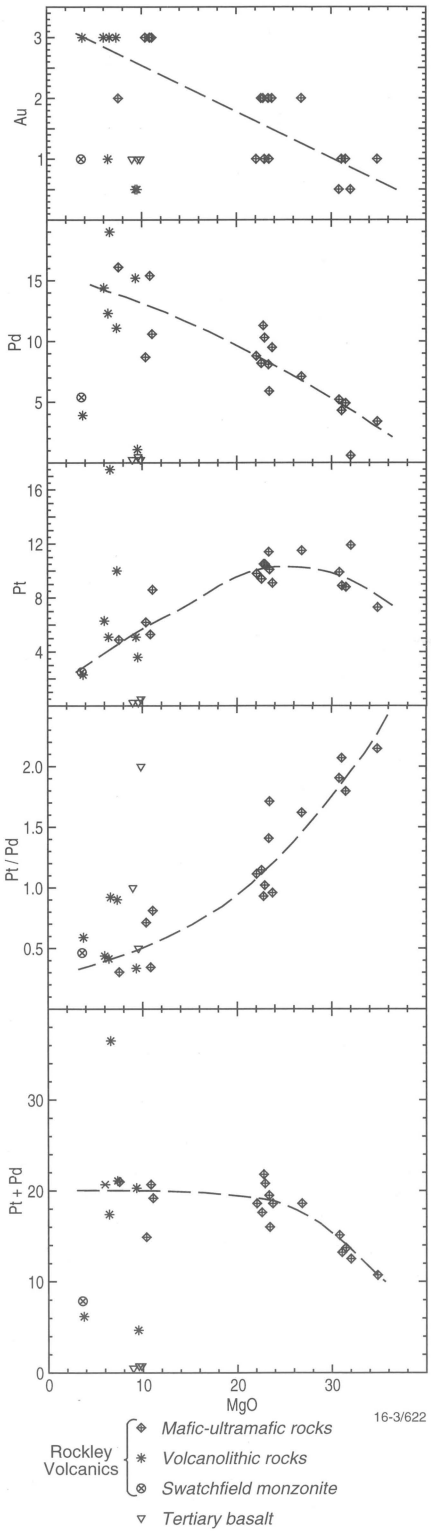

Fig. 16. Relationships between Pt, Pd, and Au (in parts per billion) and fractionation represented by MgO (weight per cent) for suites of samples from the Rockley Volcanics and Tertiary basalts from the Oberon 1:100 000 Sheet area.

Chrome-spinel is an important accessory mineral in the ultramafic rocks (Cr contents 2000–3400 ppm), but is absent from or only a minor constituent of the more basaltic non-cumulus rocks. A correlation between Pt and Cr in ultramafic cumulates and less magnesian rocks suggests that chrome-spinel could be a factor controlling the concentration of Pt (Fig. 17). A close relationship between Pt and chrome-spinel is also suggested by experiments carried out by Capobianco & Drake (1990: Geochemica et Cosmochimica Acta, 54, 869–874), which — although they excluded data on Pt — highlighted the incompatibility of Pd in spinel and the high compatibility of Rh and Ru in this mineral.

PGEs in the Rockley Volcanics can amount to about 20 times their concentrations in 'normal' basaltic assemblages, as exemplified by the Tertiary volcanics, and reflect the typically high concentrations of these elements in Ordovician shoshonites elsewhere in the central Lachlan Fold Belt. Pt is more highly concentrated in the ultramafic rocks, and Pd and Au increase as the rocks become more felsic. Favourable localities for Pt enrichment in the Oberon area therefore should be peridotite–pyroxenite rock assemblages, particularly those near Rockley — such as Dunns Plains and Dog Rocks. Depending on the timing of the entry of sulphur into the system, Pd and Au — on the other hand — would have been concentrated in felsic differentiates, such as the monzonite (MgO ~3.6%) identified during the NGMA mapping in the Swatchfield area south of Black Springs (Wallace & Stuart-Smith 1994: AGSO Record 1994/12). The Swatchfield monzonite (part of the Rockley Volcanics) appears to have undergone an estimated anomalous threefold depletion in Pd and Au (Fig. 16), suggesting that these elements had been extracted from the system at an earlier stage — possibly by fluid separation in a mineralising event. Pd and Au also appear to have been lost from two of the volcanolithic samples. In contrast, the anomalously high Pt and Pd volcanolithic rocks from the Shooters Hill area south of Oberon might reflect derivation from a locally enriched PGE source.

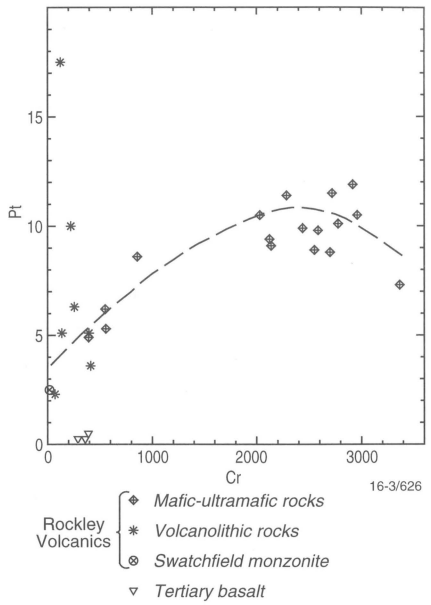

Fig. 17. Relationships between Pt (in parts per billion) and Cr (in parts per million) for suites of samples from the Rockley Volcanics and Tertiary basalts from the Oberon 1:100 000 Sheet area (symbols as for Fig. 16). The similarity of trends in this diagram and the Pt v. MgO diagram (Fig. 16) distinguishes Cr as an effective fractionation index for Pt.

No compelling evidence is suggested from the samples analysed that any significant widespread selective Au depletion occurred in the Oberon area by processes associated with burial metamorphism, as suggested by Wyborn (1988: op. cit.) for other areas. The recently completed NGMA mapping shows that a considerable proportion of Au mineralisation in the Oberon area coincided with faults. This association suggests that localised mobilisation of Au, rather than a general mobilisation of Au brought about by burial metamorphism, may be a more likely explanation for Au enrichment in Oberon. Such mobilisation of Au and PGEs from the Rockley Volcanics would have been assisted by fracturing and entry of hot S-rich fluids associated with later intrusions, as — for example — in the Lucky Draw gold deposit at Burraga (Brewer & Arundell 1994: Geological Survey of New South Wales, Report GS 1994/139). South of Black Springs, therefore, the contact aureoles of the Carboniferous Greenslopes and Isabella Granites in the outcrop of the Rockley Volcanics (particularly the Swatchfield monzonite) could be attractive for Au and Pd exploration.

[1] AGSO Division of Regional Geology & Minerals, GPO Box 378, Canberra, ACT 2601; tel +61 6 249 9582, fax +61 6 249 9983; e-mail dwallace@agso.gov.au.

Lead-isotope model ages

Continued from back page

Alternative approaches, and the age of the Broken Hill Pb–Zn ore

Applications of other approaches to obtain Pb-isotope model ages for the Proterozoic Pb–Zn ores have been less successful. For example, the plumbotectonics model of Zartman & Doe (1981: Tectonophysics, 75, 135–162) and Zartman & Haines (1988: Geochimica et Cosmochimica Acta, 52, 1327–1339) — involving mixing of four components (upper crust, lower crust, depleted mantle, and orogene) through crustal differentiation and recycling by subduction processes — tends to yield Pb model ages that are younger than the geological ages, especially for samples with low μ values. It is interesting to note that the new version (V4) of the plumbotectonics model of Zartman & Haines (1988) increases the age discrepancy. Thus, to improve the accuracy of model ages derived from a plumbotectonics model for Proterozoic Pb–Zn ores, the use of geological age control points, as we have done, is essential.

What does this imply for model ages calculated from a two-stage Pb-evolution model without geological age control?

Such model ages must accommodate large uncertainties, including estimates of the age of the Earth (4.57 to 4.47 Ga?), time of the second-stage Pb evolution, and variable μ values. Inevitably, this approach creates a broad spectrum of model ages with large uncertainties for Proterozoic Pb–Zn ores. Consequently, in order to optimise model-age calculation, input of other geological constraints is necessary.

Ehlers et al. (1996: Geological Society of Australia, Abstracts, 41, 127) adopted a different two-stage-model approach for the Broken Hill Pb–Zn ore. To establish their two-stage model, they used as their control a Pb–Pb isochron (1565 ± 22 Ma) that Gulson (1984: Economic Geology, 79, 476–490) had published for apatites from the ore lode and mine sequence. They concluded that 'this age is indistinguishable from two-stage Pb model ages of Broken Hill lode sulphides, which yield a mean age of 1574 Ma (μ = 9.7, indicative of a crustal Pb source).' On this basis they suggested that the Broken Hill orebody was concentrated during high-grade metamorphism at about 1600–1590 Ma, which was established by study of U–Pb ages of metamorphic zircon, sphene, and monazite (Gulson 1984: Economic Geology, 79, 476–490; Page & Laing 1992: Economic Geology, 87, 2138–2168). When Pb-isotope data from the Broken Hill ore (very homogeneous) and from apatites in the ore lode (CSIRO database) are plotted together, the apatite Pb–Pb isochron passes through the ore leads. This is expected for an ore lode and apatite system with extremely low $^{238}U/^{204}Pb$ (i.e., μ practically zero), and thus there was virtually no radiogenic Pb growth from the time of ore formation to the time when regional granulite-facies metamorphism at Broken Hill cooled down to the blocking temperature for the U–Pb system of apatite in the ore lode (Gulson 1984: op. cit.). Consequently, this approach will not be able to estimate the time gap between ore formation and the apatite Pb–Pb isochron age. It will not give a unique formation age for the Broken Hill Pb–Zn ore.

In contrast to the above view that the Broken Hill lode formed during high-grade metamorphism, the galena Pb and zircon U–Pb data concur with the hypothesis that the Broken Hill Pb–Zn ore is of synsedimentary, exhalative, or syndiagenetic origin, and its formation age is best represented by a zircon U–Pb age of 1690 ± 5 Ma for the Potosi Gneiss in the mine sequence (Page & Laing 1992: op. cit.). Furthermore, very low $\delta^{13}C_{PDB}$ values of about –22 per mil observed in calcite of the Broken Hill ore (e.g., Dong et al. 1987: Transactions of the Institution of Mining and Metallurgy, Section B: Applied Earth Science, 96, B15–29) imply that ore formation was associated with hydrocarbon activity in the sedimentary basin.

Table 1. Comparison of Pb model ages with geological ages (zircon U–Pb) of host sequences of Early Proterozoic VMS, an Early Proterozoic granite, and mid-Proterozoic sediment-hosted Pb–Zn ores

Deposit	*U–Pb age Ma*	*Model age Ma*	*Reference for zircon U–Pb age*
Flin Flon VMS	1886	1880	Gordon et al. 1990: Geological Association of Canada, Special Paper, 37, 177–199
Wisconsin VMS	1860	1875–1820	Afifa et al. 1984: Economic Geology, 79, 338-353
Koongie Park VMS	1840	1820	Page et al. 1994: AGSO Research Newsletter, 20, 5–7
Cullen Batholith	1825	1830	Stuart-Smith et al. 1993: AGSO Bulletin 229
Broken Hill	1690	1675	Page & Laing 1992: Economic Geology, 87, 2138–2168
Mount Isa	1652	1653	Page & Sweet in press: Australian Journal of Earth Sciences
HYC	1640	1640	Page & Sweet in press: op. cit.
Century	1595	1575	Page & Sweet in press: op. cit.

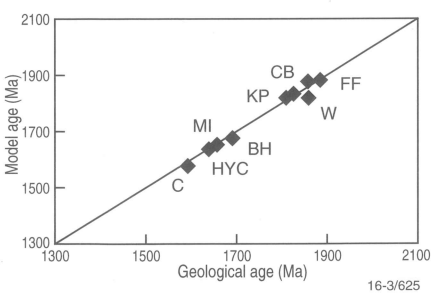

Fig. 18. Comparison of Pb-isotope model ages with zircon U–Pb ages of the host sequences for some Early Proterozoic VMS and sediment-hosted Pb–Zn deposits. Letter symbols are the same as in Figure 19.

Anomalous Pb model ages, and implications for the source rocks

Lead model ages and respective geological ages are sometimes grossly discrepant. Such discordances in model-age estimation, when evaluated together with information from the regional geology, can offer useful insights into source-rock characteristics. For example, as shown in Figure 18 and Table 1, the Pb model age for the Koongie Park VMS mineralisation — about 20 km southwest of Halls Creek, in the East Kimberley (WA) — agrees well with the zircon age of the host Koongie Park Formation, dated at 1843 ± 2 Ma (Page et al. 1994: AGSO Research Newsletter, 20, 5–7). In contrast, Pb model ages for Cu–Pb–Zn mineralisation at Little Mount Isa and Ilmars, about 30 km northeast of Halls Creek, hosted in ~1880-Ma Biscay Formation (Hoatson et al. 1995: AGSO Research Newsletter, 22, 1–2), are anomalous (2200–2300 Ma). A viable explanation for these anomalous Pb model ages is that their source region has an Archaean age, and has experienced retarded Pb-isotope evolution in a long-term low-μ environment caused by U loss during Archaean high-grade metamorphism. This possibility can be further evaluated by data on the $^{208}Pb/^{204}Pb$ versus $^{206}Pb/^{204}Pb$ plot (Fig. 19b). As Th is less mobile than U during high-grade metamorphism it will produce a 'normal' amount of decay product ^{208}Pb. Data in Figure 19b show that $^{208}Pb/^{204}Pb$ values for Little Mount Isa and Ilmars ores lie far above the growth curve, but are similar to that for the Koongie Park VMS. Thus, Pb-isotope data for these anomalous samples provide further strong, albeit circumstantial, evidence for the existence of Archaean basement in the Halls Creek region of the East Kimberley.

[1] AGSO Division of Regional Geology & Minerals, PO Box 378, Canberra, ACT 2601; tel. +61 6 249 9484 (S-sS); tel. and fax +61 6 249 4261 (RWP); fax +61 6 249 9983 (S-sS); e-mail ssun@agso.gov.au, rpage@agso.gov.au.

[2] Division of Exploration & Mining, CSIRO, 51Dehli Road, North Ryde, NSW 2113; tel. +61 2 887 8712; fax +61 2 887 8183; e-mail g.carr@dem.csiro.au.

A continued effort to improve lead-isotope model ages

Shen-su Sun[1], Graham R. Carr[2], & Rodney W. Page[1]

Dating the formation ages of metamorphosed and deformed Proterozoic sediment-hosted, massive Pb–Zn sulphide ores is an important issue relevant to ore genesis and exploration strategy. Zircon U–Pb dating of tuffaceous beds in or close to ore-bearing sequences is a direct way of obtaining the formation ages. However, continuing debates challenge both the authenticity of some of the 'tuffaceous beds' studied, and the evidence for the syngenetic-versus-epigenetic origin of these sediment-hosted Pb–Zn ores. An independent approach to these issues is to use the improved Pb-isotope model ages of orebodies as a check on the reliability of the zircon U–Pb ages of 'tuffaceous beds' and other geological criteria. Once an internal consistency is obtained, these ore-formation ages can then be integrated with other field-based information to develop more sophisticated ore-genetic models.

Our new developments

In a previous article (Sun et al. 1994: AGSO Research Newsletter 20, 1–2), we proposed the use of local zircon age control points to calibrate Pb-isotope model ages. An ideal candidate as a control point in the Early Proterozoic of northern Australia is the HYC Pb–Zn deposit. Recent work by Dr Mark Hinman (currently at Mount Isa Mines Ltd) on the HYC orebody (Hinman 1995: AGSO Record 1995/5; Hinman et al. 1994: Geological Society of Australia, Abstracts, 37, 176) justifies our past use of the HYC as a control point. Detailed structural, petrological, and geochemical studies of HYC in both an ore-deposit and a regional context strongly support a syndiagenetic to synsedimentary origin in which the ore formed mainly within 10–20 m below the sediment–water interface. SHRIMP zircon U–Pb dating of tuffaceous beds in the McArthur Group close to the mineralised rock in the Barney Creek Formation indicate that the age of deposition is 1640 ± 3 Ma (Page & Sweet in press: Australian Journal of Earth Sciences). AGSO's ongoing SHRIMP zircon U–Pb study of several other tuffaceous beds in the McArthur Group indicates stratigraphically consistent results.

If the formation age of HYC is assumed to be 1640 Ma, as shown in Figure 19a, Pb model ages for other Early Proterozoic sediment-hosted Pb–Zn ores in northern Australia with similar μ values (i.e., close to the growth curve in Figure 19a) can be estimated quite accurately. Within a short time span of ~100 Ma, the model ages are almost independent of choice between the two-stage Pb-evolution model (Stacey & Kramers 1975: Earth & Planetary Science Letters, 26, 207–221), the continuous-growth-of-μ model (Cumming & Richards 1975: Earth & Planetary Science Letters, 28, 155–171), and other models. The Pb model age of Mount Isa Pb–Zn ore is definitely older than the HYC by 13–14 Ma, and thus is 1653–1654 Ma. This model age agrees very well with the zircon U–Pb age of 1652 ± 7 Ma for a tuff bed in the Urquhart Shale in the ore sequence (Page & Sweet in press: op. cit.). Such agreement is consistent with a synsedimentary or diagenetic origin for the Mount Isa Pb–Zn ore.

In a broader picture, as shown in Table 1 and Figure 18, it is somewhat surprising to find that this HYC-based model seems also to work well for the Broken Hill Pb–Zn ore and for some Early Proterozoic volcanogenic massive sulphide (VMS) deposits — notably from Koongie Park (Northern Territory), northern Wisconsin (USA), and the Flin Flon belt (Canada) — for which there is a good correlation between Pb model ages and geological ages.

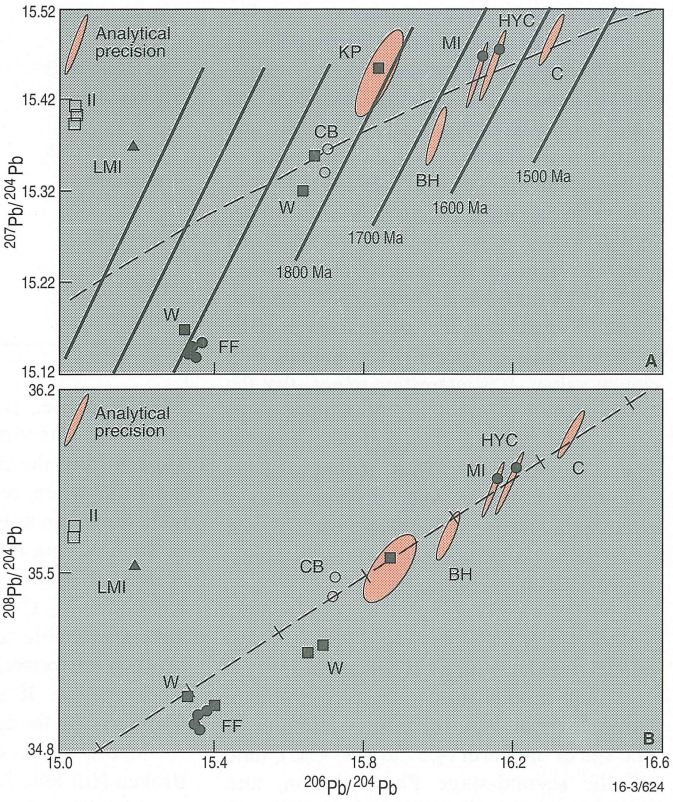

Fig. 19. Lead-isotope-ratio plots for major Australian Early Proterozoic Pb–Zn deposits: (A) $^{207}Pb/^{204}Pb$ versus $^{206}Pb/^{204}Pb$; (B) $^{208}Pb/^{204}Pb$ versus $^{206}Pb/^{204}Pb$. Model-age isochrons are constructed from the continuous-growth-of-μ model (Cumming & Richards 1975: op. cit.), for which the HYC formation age of 1640 Ma is a control point. Error ellipsoids shown in the upper left corners represent ± 0.05% per mass difference. Our new data for HYC and Mount Isa collected by the double-spike method are shown as black circles associated with data ellipsoids. BH = Broken Hill, C= Century, CB = Cullen Batholith feldspar (open circles), FF = Flin Flon VMS (Canada), KP = Koongie Park VMS, Il = Ilmars, LMI = Little Mount Isa, MI = Mount Isa, W = Wisconsin VMS (USA). The spread of Wisconsin data is represented by the four black squares.

Another way to derive better Pb-isotope model ages is to apply the ^{207}Pb–^{204}Pb double-spike method (e.g., Compston & Oversby 1969: Journal of Geophysical Research, 74, 4338–4348; Woodhead et al. 1995: Analyst, 120, 35–39) and obtain large and stable signals during mass spectrometric analysis. New Pb-isotope data collected this way for the HYC and Mount Isa Pb–Zn ores have much better quality than those reported in the literature. Uncertainties in isotope ratios associated with mass spectrometric analysis have been greatly reduced from about ± 0.1 to ± 0.01 per cent. Since errors in $^{206}Pb/^{204}Pb$ and $^{207}Pb/^{204}Pb$ are correlated by mass fractionation effects, and the error ellipsoid is roughly parallel to the isochron (Fig. 19a), the uncertainty in the model age derived from the double-spike method is much less than ~0.8 Ma associated with the $^{206}Pb/^{204}Pb$ analytical uncertainty of 0.01%. Thus, very small, relative Pb-isotope variations can be revealed by using the double-spike method.

Continued on p. 19

AGSO AUSTRALIAN GEOLOGICAL SURVEY ORGANISATION

The AGSO Research Newsletter is published twice a year, in May and November. For further information, please contact AGSO's Public Relations & Marketing Section, tel. +61 6 249 9111 (extn 9623), fax +61 6 249 9982. Correspondence relating to the AGSO Research Newsletter should be addressed to Geoff Bladon, Editor, AGSO Research Newsletter, Australian Geological Survey Organisation, GPO Box 378, cnr Constitution Avenue & Anzac Parade, Parkes, Canberra, ACT 2601; tel. +61 6 249 9111 (extn 9249), fax +61 6 249 9990, e-mail gbladon@agso.gov.au.
 ISSN 1039-091X PP255003/00266